AD-781 688

DYNAMIC MAGNETOELASTIC PROPERTIES OF RARE-EARTH MATERIALS

Paul L. Donoho, et al

Rice University

Prepared for:

Army Missile Command
Advanced Research Projects Agency

30 June 1974

DYNAMIC MAGNETOELASTIC PROPERTIES OF RARE-EARTH MATERIALS

FINAL REPORT

November 5, 1971 - November 30, 1973

MATERIALS SCIENCE LABORATORY

WILLIAM MARSH RICE UNIVERSITY

HOUSTON, TEXAS 77001

PAUL L. DONOHO

FRANZ R. BROTZEN

KAMEL SALAMA

WAYNE C. HUBBELL

WORK SUPPORTED BY DOD CONTRACT NO. DAAH01-72-C-0285

Effective Date: November 5, 1971

Expiration Date: November 30, 1973

Contract Amount: $206,487.00

Program Code: A 3168Z

MONITORED BY U.S. ARMY MISSILE COMMAND, R. L. NORMAN, PROJECT MANAGER

SPONSORED BY

ADVANCED RESEARCH PROJECTS AGENCY

ARPA ORDER NO. 1685

Security Classification

DOCUMENT CONTROL DATA - R & D AD 781 688

(Security classification of title, body of abstract and indexing annotation must be entered when the overall report is classified)

1. ORIGINATING ACTIVITY (Corporate author)

Rice University
Materials Science Laboratory
Houston, Texas 77001

2a. REPORT SECURITY CLASSIFICATION

Unclassified

2b. GROUP

3. REPORT TITLE

Dynamic Magnetoelastic Properties of Rare-Earth Materials

4. DESCRIPTIVE NOTES (Type of report and inclusive dates)

Final Report 2 November 1970-1 November 1971

5. AUTHOR(S) (First name, middle initial, last name)

Paul L. Donoho, Franz R. Brotzen, Kamel Salama, and
Wayne C. Hubbell

6. REPORT DATE	7a. TOTAL NO. OF PAGES	7b. NO. OF REFS
June 30, 1974	66	38

8a. CONTRACT OR GRANT NO.	9a. ORIGINATOR'S REPORT NUMBER(S)
DAAH01-72-C-0285	
b. PROJECT NO.	
c.	9b. OTHER REPORT NO(S) (Any other numbers that may be assigned this report)
d.	

10. DISTRIBUTION STATEMENT

Distribution of this document is unlimited.

11. SUPPLEMENTARY NOTES	12. SPONSORING MILITARY ACTIVITY
	Advanced Research Projects Agency, Arlington, Virginia 22209

13. ABSTRACT

Summary of the goals and accomplishments of a research program on the dynamic magnetoelastic properties of rare-earth materials. Both elastic wave propagation and elastic-wave ultrasonic generation were investigated in pure rare-earth metals and in terbium-iron compounds.

DD FORM 1 NOV 1473

Unclassified

Security Classification

14 KEY WORDS	LINK A		LINK B		LINK C	
	ROLE	WT	ROLE	WT	ROLE	WT
Rare Earths						
Elements and Compounds						
Magnetic Properties						
Magnetostriction						
Ultrasonic Transducers						
Ultrasonic Propagation						

ABSTRACT

This report presents a summary of the research goals and accomplishments of a program concerned with the dynamic magnetoelastic properties of materials containing rare-earth elements. Results are presented for two main classes of phenomena: first, the effects of magnetoelastic interactions on the propagation of elastice waves through rare-earth materials, and second, the utilization of the magnetoelastic interaction for the generation of high-frequency ultrasonic elastic waves. Results were obtained for both the pure rare-earth elements (Gadolinium, Terbium, Dysprosium, Holmium, and Erbium) and for intermetallic compounds such as the terbium- iron cubic Laves-phase material, $TbFe_2$. Attempts were made, where possible, to interpret the experimental results in terms of theoretical models for the fundamental magnetoelastic interactions. Most of the work described here was in a preliminary state at the time this contract was terminated, and so the full analysis of the work and the ways in which it meets the goals of the contract cannot be fully made at this time.

TABLE OF CONTENTS

I. INTRODUCTION

This report describes the results of a research program on the magnetic, elastic, and magnetoelastic properties of rare-earth materials, including both the pure rare-earth elements and rare-earth-iron-group intermetallic compounds. This program has been sponsored by the Advanced Research Projects Agency of the U. S. Department of Defense, and it has been carried out under Contract No. DAAHO1-71-C-0259 (1 November 1970 - 31 October 1971) and Contract No. DAAHO1-72-C-0285 (4 November 1971 - 31 December 1973), monitored by the U. S. Army Missile Command. In this introductory section of the report, the original motivation for this program and its specific goals are reviewed, and a summary of the accomplishments attained during the course of the program is presented.

A. Motivation for Research on the Magnetoelastic Properties of Rare-Earth Materials.

As the fundamental properties of rare-earth materials first began to be revealed through many different types of experimental research, it was quickly recognized that their magnetic and magnetoelastic properties are particularly interesting, with a number of potentially important technological applications. Most of the known magnetic and magnetoelastic properties of the pure rare-earth elements and certain rare-earth alloys are described in detail in a recent book edited by Elliott[1], and a compilation of many fundamental magnetic and magnetoelastic properties of a number of rare-earth materials is given by Tebble and Craik[2]. Both of these works provide extensive bibliographies of the original literature in the area of rare-earth magnetism.

One of the most unusual magnetic properties of the heavy rare-earth elements (Gd, Tb, Dy, Ho, Er, and Tm) is the existence of several types of periodic magnetic ordering, including both ferremagnetic and antiferromagnetic phases. Examples of this periodic ordering are shown schematically in Fig. 1. All of these elements possess a hexagonal close-packed crystal structure (hcp) which can be considered to be composed of basal-plane layers of trivalent ions perpendicular to the hexagonal-symmetry axis (c-axis). In all the observed periodic ordering structures, all the ions in a given basal-plane layer are ferromagnetically aligned, but the direction of the magnetic moment of a basal-plane layer changes

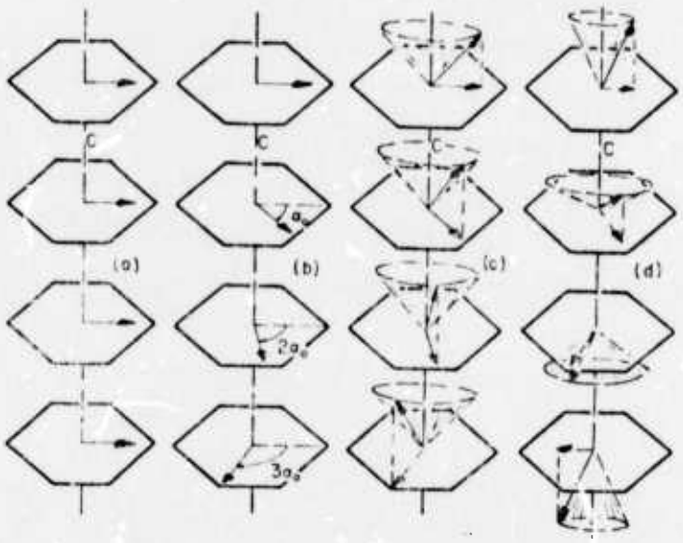

Fig. 1 Magnetic Ordering Arrangements of the Rare-Earth Elements

in a periodic fashion from one layer to the next. For example, in the case of Dy in its antiferromagnetic phase (85 K < T < 179 K), the ordering has been described as helicoidal, with the moment of each basal-plane layer lying in the basal plane, but with a finite angle of rotation of the magnetic moment from one layer to the next, as indicated in Fig. 1.

The periodic magnetic ordering in these rare-earth elements arises from the nature of the exchange interaction between rare-earth ions, an indirect interaction in which the conduction electrons play an essential part. This indirect exchange interaction may be envisioned as one in which a rare-earth ion interacts, through the normal electrostatic exchange interaction, with the conduction electrons at the Fermi surface, leading to a spin polarization of the sea of conduction electrons in the vicinity of the rare-earth ion. This spin polarization extends through the crystal as a spin-density wave, with a wavelength characteristic of the electronic wavelength for electrons at the Fermi energy. The conduction electrons then undergo direct exchange interactions with neighboring rare-earth ions, and it has been shown[1] that the net interaction between two rare-earth ions is such that it can be described by means of a Heisenberg exchange operator. Because, however, the electron polarization produced by the interaction with the first rare-earth ion oscillates spatially in a wavelike fashion, the interaction

between two neighboring rare-earth ions may be either ferromagnetic or antiferromagnetic, depending upon their spatial separation. It is the competition between antiferromagnetic and ferromagnetic exchange among all pairs of ions in the crystal which leads to periodic magnetic ordering. The actual type of ordering, however, is a result of both the exchange interactions and the magnetic anisotropy of a particular material.

Although the phenomenon of periodic ordering associated with the pure rare-earth elements and many of their alloys and compounds is in itself quite interesting, it does not constitute the principal point of interest from the standpoint of the potential technological applications of rare-earth materials which are the subject of the research program described here. The periodic ordering found in many of these materials does, however, play an important part in the determination of many other observable properties of interest, and it must, of course, be carefully taken into account when it occurs.

Most of the properties of interest for the present research program are connected with the very large magnetocrystalline anisotropy exhibited by most magnetically ordered rare-earth materials and with the dependence of this anisotropy on the state of strain of the crystal lattice. The strain dependence of the anisotropy leads, of course, to the phenomenon of magnetostriction. Although an appreciable fraction of the overall magnetic anisotropy of rare-earth magnetic materials arises from the anisotropic nature of the exchange interaction itself, the most important contribution arises from the interaction of each rare-earth ions with the crystalline electric field produced by the neighboring ions. Although the crystalline electric field is small in metals, because of the shielding effect of the conduction electrons, its effect on the orientation of the angular momentum of a rare-earth ion is quite large. The electrons responsible for the magnetic moment of a rare-earth ion lie in the f-shell, highly localized deep within the ion and shielded from the environment by filled outer s- and p-shells. Because the f-electrons retain very closely the same character in a crystalline environment as that found in free ions, the electronic charge distribution of the f-shell of a rare-earth ion is highly anisotropic. Consequently, the free energy associated with each ion in a crystal depends strongly upon the orientation of the angular-momentum vector of the ion with respect to the crystallographic principal axes associated with the crystalline electric field. Thus, the magnetic properties of rare-earth materials are nearly always highly anisotropic, with effective uniaxial anisotropy fields as large as several hundreds of kilogauss.

The extremely large anisotropy of the rare-earth materials has led to the development of a new class of rare-earth-cobalt permanent magnets with very large coercive force and high remanent magnetization[3]. For the research program described here, however, it is not so much the magnitude of the anisotropy energy that is of interest as it is the dependence of this anisotropy energy upon the state of lattice strain.

Because the magnetic anisotropy depends largely upon the crystal field produced by the ions in the neighborhood of a given lattice site, and because the magnitude and symmetry of this crystal field depend strongly upon the state of strain of the lattice with respect to its normal unstrained state, the overall free energy, a combination of the anisotropy energy and the elastic energy, may reach a minimum for a finite value of the lattice strain tensor, leading to the phenomenon of magnetostriction. In the case of many rare-earth materials, the observed magnetostrictive strain can be as large as several orders of magnitude greater than that observed in most iron-group magnetic materials. This extremely large magnetostriction, manifested by magnetostrictive strain as large as nearly one per cent in some materials[1], is the property of rare-earth materials which has motivated most of the research program described here. The fact that the magnetostriction observed in many rare-earth materials is many times larger than that of most other magnetostrictive materials suggests the possibility that rare-earth materials may provide a new class of materials suitable for applications as magnetostrictive ultrasonic transducers of high efficiency. Such transducers, capable of the generation of high-intensity, high-frequency, sound waves might be expected to lead to significant improvement in the development of sonar transducers and in the area of materials testing and processing. Most of the work described here has been directed toward the obtaining of a better understanding of magnetoelastic effects in rare-earth materials, particularly in the case of dynamic magnetoelastic strain, and toward the development of high-frequency ultrasonic transducers utilizing rare-earth materials.

In addition to the possible application of the large magnetostriction of rare-earth materials in the development of highly efficient ultrasonic transducers, work on the general magnetoelastic properties may prove useful in providing information of importance in the development of rare-earth permanent magnets[3] and in the development of rare-earth-iron-group magnetic bubble-domain memory and logic elements[4]. Furthermore, rare-earth materials may find useful applications, as a result of some of the work described here, as acoustic circuit elements in

high-frequency signal-processing systems employing both bulk and surface acoustic waves.

B. Objectives of the Research Program

In the initial proposal which led to the funding of this research program by the Advanced Research Projects Agency, the principal objective was the development of highly efficient high-frequency magnetostrictive ultrasonic transducers utilizing rare-earth materials. Although it was realized that the pure rare-earth elements, which are strongly magnetostrictive only below their magnetic transition temperatures, nearly all of which are in the cryogenic range, would probably not be useful in many applications where the cryogenic temperatures required for their operation as transducers would be unacceptable, it was initially proposed to concentrate a considerable effort on transducers fabricated from these elements in order to learns as much as possible concerning dynamic magnetoelastic effects at high frequencies in rare-earth materials. The ultimate goal, of course, was to find new materials with large magnetostriction at room temperature and above. Such materials were unavailable at the beginning of this program, but in 1971 Clark and Belson[5] reported the observation of very large magnetostriction in polycrystalline $TbFe_2$ and other rare-earth-iron intermetallic compounds. From that point in time, the research carried out in this program on the development of magnetostrictive ultrasonic transducers was concentrated on these new materials.

In addition to work on the development of ultrasonic transducers, it was apparent from the inception of this research program that it would be necessary to obtain information concerning a number of fundamental properties of rare-earth materials related to the dynamic magnetoelastic effects of primary interest. In particular, the effects of magnetoelastic interactions on the characteristics of elastic-wave propagation in rare-earth materials are important in that they are directly related to the problem of the magnetostrictive generation of ultrasonic elastic waves. Consequently, a program was initiated to obtain information on the elastic constants of the rare-earth elements, with emphasis on the magnetoelastic contributions to these elastic constants, and on elastic-wave attenuation at high frequencies in the rare-earth elements. At the same time, a theoretical analysis of the problem of magnetoelastic effects on elastic-wave propagation was developed in order to permit a satisfactory analysis of the experimental results in terms

of established theoretical models of the static magnetic and magnetoelastic properties of rare-earth materials. This theoretical treatment of dynamic magnetoelastic effects in rare-earth materials was also formulated in such a way as to permit the prediction of the characteristics of magnetostrictive ultrasonic generation in these materials, but it was limited to the case of single-crystal specimens.

Other experimental programs were developed as the overall program progressed, for the purpose of correlating static magnetic and magnetoelastic properties of rare-earth materials with their dynamic magnetoelastic properties. One of these programs concerned the measurement of the magnetization of thin-film specimens of the materials used for the fabrication of thin-film ultrasonic transducers. It was discovered very early in the use of $TbFe_2$ for ultrasonic transducers that the properties of this material in the form of thin films are quite different from the reported bulk properties. Consequently, a sensitive vibrating-sample magnetometer was constructed for the purpose of measuring the magnetization of films deposited on various substrates under a wide range of deposition conditions. Another program concerned the measurement of the magnetostriction of thin-film specimens and very small single-crystal specimens of rare-earth-iron-group intermetallic compounds such as $TbFe_2$. A system utilizing the method of holographic interferometry was developed for this purpose, because it was believed that only such a method would permit the measurement of the magnetostriction of fragile and brittle thin films of rare-earth materials.

C. Principal Accomplishments of the Research Program

The major accomplishments of this research program on the magnetoelastic properties of rare-earth materials are summarized briefly here. A more detailed description of each area is given in the main body of this report which follows.

1. Magnetostrictive Ultrasonic Generation: Magnetostrictive ultrasonic generation was demonstrated in thin-film transducers of several pure rare-earth elements, namely Gd, Tb, Ho, Dy, Er, and in thin-film transducers of $TbFe_2$ and other rare-earth-iron intermetallic compounds. In the case of the pure elements, particularly Dy at liquid-helium temperatures, very strong ultrasonic generation at frequencies up to 1,550 MHz was observed, with efficiencies of generation some 30 dB better than that observed in the case of piezoelectric generation in single-crystal quartz under the same experimental conditions. As expected, however, magnetostrictive ultrasonic generation could not be observed at temperatures above

the magnetic ordering temperatures of these elements. One exception occurred, however, in the case of Tb, in which ultrasonic generation was observed at temperatures in the paramagnetic range ($T > 230$ K). In this case, however, the ultrasonic intensity was fairly small. Some ultrasonic generation was observed at frequencies as high as 10 GHz, but only at very low temperatures, due to the large attenuation of elastic waves of this high frequency at temperatures above 20-30 K in most materials. Because of the interest in developing transducers of high efficiency capable of operation at room temperature and above, work on transducers fabricated from the pure rare-earth elements was not continued after it became evident that the rare-earth-iron intermetallic compounds were considerably more promising. Nevertheless, as described more fully in the following section, a gret amount of useful information concerning ultrasonic generation in the rare-earth elements was obtained. Although it was originally planned to investigate magnetostrictive ultrasonic generation in single-crystal specimens of the pure rare-earth elements, it was not possible to obtain results in this area during the time span of this program.

The most interesting results were obtained in the case of magnetostrictive ultrasonic generation in thin-film transducers fabricated from the intermetallic compound $TbFe_2$. As mentioned above, Clark and Belson[5] found that this material in bulk form possesses a very large static magnetostriction at room temperature in polycrystalline form. This result is in strong contrast to the case of the pure rare-earth elements, for which, even in highly magnetically ordered states at low temperatures, large magnetostriction is found only in single-crystal specimens. Thin-film transducers evaporated onto single-crystal quartz substrates were fabricated in this program, and it was quickly found that strong magnetostrictive ultrasonic generation occurs at frequencies as high as 1,550 MHz. Only shear-wave generation was observed, a result accounted for by the theoretical model presented in a subsequent section, but the intensity of the ultrasonic waves generated magnetostrictively was some 20 dB greater than that of piezoelectrically generated longitudinal waves in single-crystal quartz and, perhaps, 30 dB greater than that of piezoelectrically generated shear waves at the same temperature and frequency.

An unexpected but highly interesting result of the investigation of magnetostrictive ultrasonic generation in thin films of $TbFe_2$ was the occurrence of a very large hysteresis in the field dependence of the ultrasonic intensity. After initial magnetization to saturation in an applied field of approximately 20 kG,

the film still exhibited strong ultrasonic generation when the field was removed. An examination of the film magnetization using a vibrating-sample magnetometer revealed that the film acts as a permanent magnet, with a coercive force of approximately 4 kOe at room temperature and a remanent magnetization of approximately 80 per cent of the saturation value. This thin-film behavior is in strong contrast to that of bulk $TbFe_2$, which exhibits fairly small hysteresis, with a correspondingly small coercive force and remanence. Although this interesting behavior is not understood at present, it is perhaps due to the occurrence of some degree of crystallographic ordering in the film during the deposition procedure. One interesting possible application of this large coercive force and remanence is the development of thin-film permanent magnets which may be useful in magnetic bubble-domain memory and logic systems requiring permanent bias fields over a very small volume.

At the time of writing this report, work is still in progress on the properties of thin-film ultrasonic transducers fabricated from $TbFe_2$ and other rare-earth-iron compounds. The effects of variation of the deposition parameters, film thickness, composition, and the effects of post-deposition annealing are being systematically studied. Because of the totally unexpected hysteresis encountered in the work described above, an investigation, using the method of holographic interferometry described in a subsequent section of this report, of the static magnetostriction of thin films, both free and bonded to a substrate, is under way. Since the magnetization exhibits such unusual properties when $TbFe_2$ is produced in the form of a thin film, it is likely that other magnetic and magnetoelastic properties of this material will also be quite different from their bulk behavior.

2. Elastic-Wave Propagation in Rare-Earth Materials: As mentioned above, an extensive program of the investigation of the behavior of both the elastic-wave velocities and elastic-wave attenuation in rare-earth materials was carried out under the overall research program. Studies were carried out on single-crystal specimens of the pure rare-earth elements Tb, Dy, Ho, and Er, and, in addition to providing in the cases of Tb, Ho, and Er new information on the elastic constants of these elements over wide temperature ranges, this work yielded a number of interesting and useful results concerning magnetoelastic effects on the behavior of elastic waves at high frequencies in rare-earth materials. In particular, both linear and circular magnetoacoustic birefringence was observed in these materials, in accordance with the predictions of the theory described in the fol-

lowing section. These birefringence results permit the determination of certain of the shear magnetoelastic coupling constants of rare-earth materials in a manner not possible without considerable difficulty by other means, and, more important, they permit this determination at frequencies and temperatures of interest for magnetostrictive ultrasonic generation. It is the shear magnetoelastic couplings which are of greatest importance for the magnetostrictive generation of ultrasonic waves at high frequencies. The observed birefringence effects also lead to the possibility of the development of acoustic circuit elements with non-reciprocal properties, such as isolators and circulators.

It was also observed in some cases that elastic-wave velocities could be varied by as much as 7-8 per cent by the application of a magnetic field under appropriate conditions. Such an effect may be useful in the development of simple acoustic variable delay lines. In other cases, strong field-dependent ultrasonic attenuation was observed, leading to the possibility that simple acoustic variable attenuators could be developed using rare-earth materials.

Many of the results obtained in this part of the program could be analyzed by means of straightforward theoretical models of dynamic magnetoelastic interactions, including one presented in the following section and a theory developed by Southern and Goodings [6]. The results of this theoretical analysis indicate quite good agreement between theory and experiment in the area of dynamic magnetoelastic interactions in rare-earth materials, and, particularly, they show that measurements on the propagation of elastic waves in such materials may provide the best way to determine completely the quantities which characterize the magnetoelastic interactions which can occur.

3. Holographic Measurement of Magnetostriction: A system for the measurement of static magnetostriction in rare-earth materials employing the method of real-time holographic interferometry was developed to permit measurements in specimens of rare-earth materials whose configuration would not permit the use of more conventional methods for the measurement of magnetostriction. Such configurations include thin-film specimens whose magnetostriction may deviate, as discussed above, strongly from that of the same material in bulk form, and they include the very small single-crystal specimens which can be produced from rare-earth-iron compounds. After the confirmation that the holographic method does indeed give results in good agreement with those obtained by conventional methods (for specimens which permit the use of, for example, strain-gauge methods), an

attempt was made to apply this method to the case of thin films of $TbFe_2$ and to the case of a small single crystal of $ErFe_2$ which was grown for this purpose. Because of the fragility of the thin films, it has not yet been possible to obtain results in this area. However, an extensive set of results on the static magnetostriction of the single-crystal specimen were successfully obtained. When these results showed considerable disagreement with those reported (and confirmed in this work) for polycrystalline $ErFe_2$, the crystal was examined by the method of X-ray fluorescence, using an electron microprobe for excitation, in order to determine its composition. Despite the fact that the crystal had been prepared from material for which the stated purity of the erbium component was 99 per cent, according to the commercial supplier, it was found that the crystal was, in fact, a mixture of $ErFe_2$ and $TbFe_2$, with roughly comparable amounts of Er and Tb. Thus, the crystal should not have been expected to give results agreeing with what was approximately expected for pure $ErFe_2$. Numerous cross checks did, however, confirm that the magnetostriction was measured accurately, and the result of the investigation indicates that this $Tb_xEr_{1-x}Fe_2$ crystal exhibits room temperature magnetostriction somewhat large than had been reported by Clark and Belson[5] for polycrystalline $TbFe_2$. The analysis of the results is in progress, and an attempt to grow a second $ErFe_2$ crystal using material of known high purity is under way. Work is also continuing on the effort to measure the static magnetostriction of thin-film $TbFe_2$ in order to perhaps obtain a better understanding of the permanent magnet-like behavior of these films.

4. Theoretical Analysis of Dynamic Magnetoelastic Effects: When this program began, very little attention had been given to the theory of dynamic magnetoelastic effects in rare-earth materials. A general theory of static magnetoelastic effects developed by Callen and Callen[7] was at that time well established, and its predictions agreed quite well with many experimentally determined magnetoelastic properties of rare-earth materials, but the only attempts to explain dynamic magnetoelastic effects in these materials up to that point in time[8,9] had largely been nased upon earlier theoretical models developed for application to iron-group materials. It was, thus, recognized at the outset of this program that a new approach was needed in this area, extending the theory of Callen and Callen to include dynamic magnetoelastic effects and adding to the established theory where necessary. Other researchers began to attack the problem at the same time. Freyne[10] developed a thermodynamic approach to explain certain

aspects of the anomalous temperature dependence of the elastic constants of Gd, and Southern and Goodings[11,12] developed a somewhat more general theory of the magnetoelastic contributions to the elastic constants of rare-earth materials. The work of Southern and Goodings is particularly important, since these authors took account of the intrinsic nonlinear nature of elastic strain and also developed a rotationally invariant model of the magnetoelastic interaction, including terms which are important in the case of dynamic elastic strain but which had been neglected in earlier treatments of static magnetoelastic effects.

In the present work, as described in the following section, a theory of dynamic magnetoelastic interactions in rare-earth materials has been developed in a way which combines parts of the work of Freyne[10] and that of Southern and Goodings[11,12]. This theoretical treatment has been applied to explain satisfactorily certain of the experimental results reported here, and it is shown in the following section how it can be extended to apply to many more magnetoelastic phenomena.

D. Summary of the Program and Its Overall Effectiveness

In some ways, the research program discussed here accomplished its overall objectives satisfactorily, but there were also ways in which it fell short of the original goals. A number of interesting new experimental results on the dynamic magnetoelastic properties of rare-earth materials were obtained and reported in the literature and at technical conferences, and, in particular, it was shown that the intermetallic compound $TbFe_2$ is, as expected, a very promising material for the development of room-temperature magnetostrictive ultrasonic transducers. The time available for this program did not, however, permit the completion of all the individual research projects of interest. Much work remains to be done on the complete characterization of $TbFe_2$ and other rare-earth-iron intermetallic compounds as magnetostrictive ultrasonic transducers. For example, time did not permit the investigation of the effects of varying the thickness of the transducer films, of deposition in an applied magnetic field, or of post-deposition annealing of the films. Nor was it possible to investigate the properties of a wide range of film compositions.

Further work on the theory of dynamic magnetoelastic interactions, including an attempt to extend it to cover very high frequencies, is also necessary. There also remains a large body of experimental data for which there has not been time to apply the theory to explain the quantitative results. It is believed that

further extensive calculations along these lines would permit the strengthening of the theory and an overall better understanding of dynamic magnetoelastic effects in rare-earth materials.

The A.R.P.A. support of this program also ended at a time when the holographic system for the measurement of magnetostriction in thin films and very small single crystals was just beginning to yield very interesting results. It is felt that this method will very usefully supplement other methods for the measurement of static magnetoelastic effects when it reaches its full potential.

In all, it can be said that this program produced a number of interesting and useful new results, but that it ended at a time when the most interesting stage of the program had been reached. It is hoped, of course, that many of the individual projects described above and, in more detail, in what follows, can be continued with a new source of funding.

II. THEORY OF DYNAMIC MAGNETOELASTIC INTERACTIONS IN RARE-EARTH MATERIALS

Most recent attempts to develop a satisfactory theoretical model of dynamic magnetoelastic effects in rare-earth materials have been based upon the extension of the original theory of static magnetoelastic interactions in the rare-earth elements of Callen and Callen[7] to include the effects of time-dependent lattice strain. Freyne[10] employed a quasistatic thermodynamic approach to calculate the effects of the magnetoelastic interactions on the elastic constants of gadolinium, achieving quite satisfactory results. His approach is quite similar to that employed here, although the present treatment, described in detail below can be extended to cover a wider range of phenomena. Southern and Goodings[11,12] employed a quantum-field-theoretic treatment to consider the same general class of problems, obtaining in some cases results essentially in agreement with those of Freyne. The most interesting new contribution of Southern and Goodings, however, was the introduction into the Hamiltonian which serves as a model for the magnetoelastic interactions two new features. First, they took explicit account of the fact that finite strains are quadratic in the components of the tensor gradient of the lattice displacement, and, second, they took explicit account of terms in the Hamiltonian needed in order that it be rotationally invariant. In earlier treatments of static magnetoelastic effects, in which a homogeneous, uniform, strain tensor was assumed, these additional terms do not appear. They become important, however, when lattice waves of finite wavelength

are considered, and, according to Southern and Goodings[11], these additional terms lead to interesting observable effects.

The following treatment makes use of a number of ideas originated by both Freyne[10] and by Southern and Goodings[11], but it is formulated in such a way that it can in many cases be applied to the calculation of specific effects with less difficulty, and it is also useful in the calculation of magnetostrictive ultrasonic generation, a topic not considered by either Freyne or Southern and Goodings. The treatment presented here makes use of a number of simplifying approximations for the purpose of facilitating specific calculations, but many of these simplifications can undoubtedly be eliminated in cases where the added difficulty of making calculations appears warranted. The model presented here is not, therefore, intended to be a definitive treatment of the problem of dynamic magnetoelastic effects in rare-earth materials; rather, it is a model which permits semiquantitative calculations which are in some cases in quite good agreement with experimental results, and it is a model which can be improved when necessary.

A. Description of the Model for Dynamic Magnetoelastic Interactions

There is very little difference between the basic model of a system of rare-earth ions in a crystal lattice necessary for the description of dynamic effects and that which has been used by many authors for the description of static magnetoelastic effects. Much of the earlier work on static magnetic and magnetoelastic properties of rare-earth materials is summarized in the recent book edited by Elliott[1], and a more detailed treatment of magnetoelastic interactions is given by Callen and Callen[7]. The principal difference encountered in setting up a model Hamiltonian for the purpose of describing dynamic magnetoelastic effects is the necessity of allowing for strain waves of finite wavelength and for spin waves of finite wavelength. Most of the effects, however, to which the present treatment has been applied involve strain waves of wavelength much greater than the dimensions of a unit crystallographic cell, and, for the purpose of simplifying calculations, it has been assumed in most of what follows that any dynamic motion of the magnetic moments of the rare-earth ions can be described by means of a uniform-precession mode of motion. In effect, this approximation ignores the spin-wave dispersion at long wavelengths, and it is probably very well justified, since most of the effects to which the present treatment has been applied involve elastic waves of wavelength of the order of an appreciable fraction of

a millimeter. Thus, the principal additions to the usual static model Hamiltonian are simply the introduction of the lattice kinetic energy associated with strain waves of finite frequency and the introduction of the terms originated by Southern and Goodings[11] to preserve rotational invariance when the nonuniform strains associated with finite-wavelength elastic waves are considered. The additional consideration of the quadratic nature of finite strains, first considered in the context of dynamic magnetoelastic effects in rare-earth materials by Southern and Goodings, is included as well, but many of the effects treated here are not strongly dependent on the nonlinearity of the lattice strain.

The principal contributions to the model Hamiltonian are summarized in the following paragraphs:

1. Exchange Interaction: Molecular-Field Approximation

For the purposes of making relatively straightforward calculations, the usual molecular-field approximation is used here to represent the exchange interaction. Although this approximation is subject to its usual limitations and is probably not a very good approximation at very low temperatures, it is probably quite satisfactory for paramagnetic materials, which are the subject of some of the experimental work described in subsequent sections of this report, and the molecular-field approximation seems to give satisfactory results in several cases in which rare-earth materials are considered near their magnetic phase transitions. The fact that the pure rare-earth elements and many of their alloys and compounds exhibit periodic ordering structures can still be taken into account with the molecular-field approximation, if, as shown by many authors, particularly Nagamiya[13], the effective molecular field is taken to be spatially periodic in accordance with the periodic nature of the magnetization. Although it shown by several authors[14,15] that there are significant anisotropic contributions to the exchange interaction in rare-earth materials, a prediction verified by experiments on inelastic neutron scattering[16], the treatment given here does not take the anisotropic part of the exchange interaction into account except in the case of magnetoelastic interactions, as discussed below. This approximation does not, apparently, impair greatly the validity of most of the results described here.

That part of the model Hamiltonian representing the static exchange interaction can, therefore, be represented in the following way:

$$H_{ex} = \sum_n \sum_i g \mu_B \vec{H}^e_n \cdot \vec{J}_{in} \qquad \text{(II-1)}$$

In this expression, g is taken to be the free-ion Landé factor, μ_B is the Bohr magneton, $\vec{H}^e_n$ is the effective molecular field acting uniformly on all atoms of the n^{th} plane of ions perpendicular to the periodic ordering wave vector, and $\vec{J}_{in}$ is the angular-momentum operator for the i^{th} ion of the n^{th} plane. If there is no periodicity of finite wavelength in the magnetic ordering, then, of course, the effective molecular field is uniform. When periodic ordering is present, however, the effective molecular field will exhibit the same periodicity as that of the magnetization. In most calculations, the molecular field will be proportional to the magnetization or, in the case of periodic ordering, a function of the magnetic moments of a number of planes of ions. Its specific nature must be considered for each type of calculation performed.

In most of what follows, better approximations than the molecular-field approximation could undoubtedly be employed, although with a great increase in the difficulty of performing detailed calculations. In particular, for calculations involving elastic waves of very high frequencies at temperatures near the magnetic ordering transition temperature, the random-phase approximation would provide more reliable results, whereas for low-temperature calculations a fully quantized treatment of the coupled spin-wave-phonon system would be necessary. For most of the problems of interest here, however, the frequency of interest is relatively low (10-700 MHz), and resonant spin-wave-phonon interactions do not seem to be important for the determination of the characteristics of most of the experimentally observed phenomena reported here.

2. Anisotropy Energy: Crystal-Field Approximation

Although anisotropic exchange interactions undoubtedly constitute a source of magnetic anisotropy energy in many rare-earth materials[14-16], the static anisotropy will be treated, following the example of many previous authors[1], in terms of an effective Hamiltonian operator representing the interaction of each individual rare-earth ion with the electric field produced by its environment. This crystal-field approximation is undoubtedly quite satisfactory, since the f-electrons of the rare-earth ions are highly localized, but a full explanation of

certain observed magnetic ordering structures and certain features of the static magnetostriction of rare-earth elements may require the introduction of the anisotropic exchange interaction omitted here. Most of the dynamic magnetoelastic effects of interest here, however, appear to be explained adequately without the inclusion of anisotropic exchange in the static, equilibrium, terms of the model Hamiltonian.

The model Hamiltonian representing the crystal-field single-ion anisotropy can be expressed in terms of angular-momentum operator equivalents, through the use of the Wigner-Eckart theorem, as first shown by Stevens[17]. The angular-momentum tensor operators employed here are essentially the same as those used by different authors, but the normalization factors have been chosen, in some cases, differently in order to facilitate numerical calculation. The exact definition of the operators used here is given in Appendix I. For hexagonal symmetry, such as that of the hcp rare-earth elements, the appropriate model Hamiltonian is the following:

$$H_a = \sum_i P_2^0 (J_{20})_i + \sum_i P_4^0 (J_{40})_i + \sum_i P_6^0 (J_{60})_i + \sum_i P_6^6 (J_{66}^+)_i \qquad \text{(II-2)}$$

In this expression, the coefficients P_ℓ^m depend on the nature of the crystalline environment and, in principle, can be calculated. However, since most reported calculated values are not in particularly good agreement with experimentally determined values for these coefficients for most rare-earth materials[18], only the values estimated from experimental measurements are used here. In eq. (II-2) the summation is taken over all ions in the crystal, and it is assumed that each ion interacts with the lattice in the same way, so that the coefficients are identical for all ions.

Since the anisotropy free energy is an appreciable fraction of the exchange energy for many rare-earth materials, it must be taken into account explicitly in most calculations of the magnetic and magnetoelastic properties. For many purposes, however, the anisotropy energy can be represented adequately by means of only the first term of eq. (II-2), the second-degree uniaxial anisotropy term, and this truncation of the complete anisotropy model Hamiltonian will be carried out in most of the work described here, for the sake of the resulting simplification of the calculations.

3. Magnetoelastic Interactions

Two types of magnetoelastic interaction have been considered by a number of authors, following the general formalism of Callen and Callen[7]. The first type, which is designated the single-ion interaction, results from the strain dependence of the crystal field. This strain dependence produces as one effect a modification of the coefficients of the anisotropy terms of the model Hamiltonian described above, but since certain strain components reduce the point-group symmetry at each lattice site, they also introduce crystal-field terms of lower symmetry than those characteristic of the unstrained lattice. The second type of magnetoelastic interaction is the so-called two-ion interaction, which results from the strain dependence of the exchange interaction. In the usual description of this interaction[7] it is customary to include the effects of anisotropic exchange interactions although, as discussed above, they are often not taken explicitly into account in the equilibrium exchange Hamiltonian of eq. (II-1).

Both of these types of magnetoelastic interaction are considered here, although some of the calculations make explicit use of only the single-ion magnetoelastic interaction for the sake of simplifying calculations. In most cases both the single-ion and two-ion interactions lead to qualitatively similar observable effects such that it would be difficult to separate the two interactions on the basis of experimental measurements. Following Southern and Goodings[11], the treatment presented here includes both the nonlinear nature of finite strains and the added effects on the behavior of shear elastic waves resulting from the rotational invariance imposed on the magnetoelastic interaction by these authors.

a. Single-Ion Magnetoelastic Interaction

There are two principal contributions to the single-ion magnetoelastic interaction. The first is due to the strain dependence of the crystal electric field resulting from the lattice deformation due to the strain. This contribution is the one normally treated in problems involving static magnetostriction. The second contribution arises from the effective rotation of the crystal field resulting from the strain associated with shear elastic waves of finite wavelength. It is this second contribution which was introduced by Southern and Goodings[11] as a result of their imposition of rotational invariance on the model Hamiltonian, following the work of Melcher[19] and Brown[20]. Each of these contributions is con-

sidered separately in what follows.

The normal single-ion magnetoelastic interaction due to deformation of the crystal lattice as the result of a homogeneous strain would be expected to contain contributions due to the strain dependence of crystal-field terms of degree $\ell = 2$, 4, and 6, including all appropriate m-values. For the sake of simplification, however, only the terms of lowest degree, with $\ell = 2$, are included here. It would also be expected that, for each value of ℓ, terms linear in the lattice strain and higher-order strain terms should contribute to the interaction. In fact, Southern and Goodings[11] took account of a part of the higher-order strain terms by using the conventional definition of finite lattice strain, which includes terms of second degree in the particle-displacement gradient. That is, the conventional definition of strain is expressed in the following way:

$$E_{ij} = \frac{1}{2}\left[\frac{\partial u_i}{\partial x_j} + \frac{\partial u_j}{\partial x_i}\right] + \frac{1}{2}\frac{\partial u_\lambda}{\partial x_i}\frac{\partial u_\lambda}{\partial x_j} \quad . \qquad \text{(II-3)}$$

In this expression, the u_i represent the components of the vector displacement of any lattice point from its equilibrium position. The first term, in brackets, represents the usual small-signal strain tensor. This definition of strain was originally chosen to satisfy the requirement that the strain tensor represent a pure deformation of the lattice, but it is not, of course, the only tensor which can be composed of linear and quadratic combinations of the displacement gradient. In fact, such a combination would not manifestly arise in an expansion of the crystal field in terms of the displacement gradient (nor does it arise naturally in the usual expansion of the crystal lattice energy in terms of second- and third-order elastic constants). However, the strain, as defined in eq. (II-3), does provide a useful symmetric tensor for crystal-field and other expansions, with the advantage that its direct product with itself is also a tensor of higher rank. Consequently, the form of eq. (II-3) is used here, although in many cases only the small-signal, linear part of the strain need be used in a specific calculation. When only the small-signal part is used, it will be designated by the symbol ε_{ij}. In addition, it is often convenient to use the six-dimensional Voigt notation for such quantities as strain and the elastic constants. For the strain (small-signal values only), the notation e_i will be used, where the normal convention ($e_1 = \varepsilon_{11}$, $e_2 = \varepsilon_{22}$, $e_3 = \varepsilon_{33}$, $e_4 = \varepsilon_{23} + \varepsilon_{32}$, $e_5 = \varepsilon_{13} + \varepsilon_{31}$, $e_6 = \varepsilon_{12} + \varepsilon_{21}$) will be followed.

The following expression will be used as the model Hamiltonian for that part of the magnetoelastic interaction due to single-ion interactions with the crystal field, not including that part due to the rotation of the crystal field, which is treated separately below:

$$H_{me}^{I} = [\, B_1^{\alpha,2}\, E_1^{\alpha} + B_2^{\alpha,2}\, E_2^{\alpha}] \sum_i (J_{20})_i + B^{\gamma,2} \sum_i [E_1^{\gamma}(J_{22}^{+})_i + E_2^{\gamma}\,(J_{22}^{-})_i]$$

$$+ B^{\varepsilon,2} \sum_i [E_1^{\varepsilon}(J_{21}^{+})_i + E_2^{\varepsilon}(J_{21}^{-})_i] \qquad \text{(II-4)}$$

In this expression, which is valid for the hexagonal symmetry wnifh holds for the rare-earth elements, linear combinations of the cartesian strains which form the components of the various irreducible representations of the hexagonal-symmetry point group appropriate to the hcp lattice have been employed. The definitions of these quantities, denoted by the symbol E_m^{μ}, which differ slightly from those employed by Callen and Callen[7], are given in Appendix II. It should be remembered that the magnetoelastic model Hamiltonian given in eq. (II-4) ignores, for the sake of simplification, higher-order terms in both the strain and the angular-momentum tensor operators. These lowest-order terms are, however, sufficient for the description of most magnetoelastic phenomena in rare-earth materials.

That part of the magnetoelastic interaction due to the rotation of the crystal field associated with shear strain waves of finite wavelength may be treated to the same order in the following way. If a static external stress were applied to a crystal, of course, only symmetric strains, both shear and longitudinal, would result, A pure-mode shear elastic wave propagating through a crystal with finite wavelength, however, is characterized by a skew-symmetric particle-displacement gradient, and the resulting motion of the lattice may be described in terms of both a symmetric (small-signal) strain wave and an antisymmetric rotation of the coordinate system. For example, a shear wave propagating along the z-axis with its polarization along the x-axis would be characterized by a particle-displacement gradient $\partial u_x/\partial z$, which could be written as

$$\frac{\partial u_x}{\partial z} = \frac{1}{2}\left[\frac{\partial u_x}{\partial z} + \frac{\partial u_z}{\partial x}\right] + \frac{1}{2}\left[\frac{\partial u_x}{\partial z} - \frac{\partial u_z}{\partial x}\right] . \qquad \text{(II-4)}$$

Thus, following Southern and Goodings[11], a general elastic wave could be represented by a generalized strain, including both symmetric and antisymmetric parts, according to the following notation:

$$\underline{\varepsilon} = \begin{pmatrix} \varepsilon_{11} & \varepsilon_{12} & \varepsilon_{13} \\ \varepsilon_{12} & \varepsilon_{22} & \varepsilon_{23} \\ \varepsilon_{13} & \varepsilon_{23} & \varepsilon_{33} \end{pmatrix} + \begin{pmatrix} 0 & \Omega_{12} & \Omega_{13} \\ -\Omega_{12} & 0 & \Omega_{23} \\ -\Omega_{13} & -\Omega_{23} & 0 \end{pmatrix} . \qquad \text{(II-6)}$$

The symmetric part of the generalized expression in eq. (II-6) is just the small-signal strain, which is, of course, treated in the expression of eq. (II-4). The antisymmetric part is, however, equivalent to a rotation of the coordinate axes, and this rotation leads to a term in the model Hamiltonian for the single-ion magnetoelastic interaction which reflects the effect of the rotation on the anisotropy terms given in eq. (II-2). If only the second-degree anisotropy term is considered, for the sake of simplification and because the fourth- and sixth-degree terms are not included in eq. (II-4), then the following terms must be added to the single-ion magnetoelastic interaction:

$$H_{me}^{I'} = \frac{3}{2} P_2^0 \sum_i [\Omega_{13}(J_{21}^+)_i + \Omega_{23}(J_{21}^-)_i] . \qquad \text{(II-7)}$$

In the above expression, the quantities Ω_{12} and Ω_{23} are defined as follows:

$$\Omega_{13} = \frac{1}{2}\left[\frac{\partial u_x}{\partial z} - \frac{\partial u_z}{\partial x}\right] \quad ; \quad \Omega_{23} = \frac{1}{2}\left[\frac{\partial u_y}{\partial z} - \frac{\partial u_z}{\partial y}\right] . \qquad \text{(II-8)}$$

As pointed out by Southern and Goodings, this contribution to the single-ion magnetoelastic interaction should lead to observable effects in the consideration of the magnetoelastic contributions to those elastic constants associated with shear strain components.

b. Two-Ion (Exchange) Magnetoelastic Interaction

The two-ion magnetoelastic interaction arises from the strain dependence of the exchange interaction, and it can be written down to first order in the strain in the following way:

$$H_{me}^{II} = \sum_{i \neq j} H_{me}^{II}(i,j) \qquad \text{(II-9)}$$

$$H_{me}^{II}(i,j) = [D_{11ij}^{\alpha}E_1^{\alpha} + D_{21ij}^{\alpha}E_2^{\alpha}]\vec{J}_i\cdot\vec{J}_j + [D_{12ij}^{\alpha}E_1^{\alpha} + D_{22ij}^{\alpha}E_2^{\alpha}][3J_i^zJ_j^z - J(J+1)]$$
$$+ D_{ij}^{\gamma}[E_1^{\gamma}(J_i^xJ_j^x - J_i^yJ_j^y) + E_2^{\gamma}(J_i^xJ_j^y + J_i^yJ_j^x)]$$
$$+ D_{ij}^{\epsilon}[E_1^{\epsilon}(J_i^xJ_j^z + J_i^zJ_j^x) + E_2^{\epsilon}(J_i^yJ_j^z + J_i^zJ_j^y)] \quad . \qquad \text{(II-10)}$$

It should be noted that the expression for the two-ion magnetoelastic interaction given in eq. (II-10) differs from those used by Callen and Callen[7] and by Southern and Goodings[11] because of a different normalization of the strain and angular-momentum operators employed here. It might be argued that an additional term due to the rotation associated with finite-wavelength shear strain waves should also be considered here, as in the case of the single-ion magnetoelastic interaction. However, the dominant contribution to the static exchange interaction in the unstrained lattice is the isotropic Heisenberg interaction, and any anisotropic equilibrium exchange interactions have been neglected in this treatment. Only such anisotropic contributions to the exchange interaction would lead to rotational effects in the presence of shear strain waves.

The two-ion magnetoelastic interaction is easily treated within the framework of the molecular-field model, and it is included where necessary in the detailed calculations presented below. However, this interaction usually does not lead to any significant qualitative difference from results obtained through the use of the single-ion interaction alone, and, consequently, it need not always be included explicitly in specific calculations. Its importance in each case will be considered in what follows.

4. Elastic Energy--Long-Wavelength Classical Limit

The problems of interest here concern the generation and propagation of coherent elastic waves of frequencies from 10-20 MHz up to the X-band microwave range (9-10 GHz). Over this entire frequency range, the wavelength is long enough that the crystal will appear to be a continuum insofar as its effects on the wave velocity and attenuation are concerned. Thus, the purely elastic part of the problem is treated here in the low-frequency continuum limit, while the magnetic and magnetoelastic parts of the problem are treated quantum-mechanically, in the same sense as the usual semiclassical treatment of the interaction of

radiation with matter. In this approximation, the elastic potential energy may be written in the usual manner:

$$U_e = \frac{1}{2} \sum_{ijkl} c_{ijkl} E_{ij} E_{kl} + \frac{1}{3} \sum_{ijklmn} c_{ijklmn} E_{ij} E_{kl} E_{mn} + \cdots \qquad \text{(II-11)}$$

In this expression, the elastic energy is written in terms of the elastic finite strains discussed above. An exactly equivalent expression may be written in terms of the small-signal strains, with the appropriate ϵ_{ij} replacing the finite-strain E_{ij}. The only difference between the two ways of writing the elastic energy is the fact that the third-order elastic constants c_{ijklmn} will be different in the two representations (as would, of course, any elastic constants of still higher order). It should be noted that the second-order elastic constants may be defined from the above expression for the elastic energy as the second partial derivatives of the energy with respect to the strain components (in either the finite-strain or small-signal representations:

$$c_{ijkl} = \frac{\partial^2 U_e}{\partial E_{ij} \partial E_{kl}} = \frac{\partial^2 U_e}{\partial \epsilon_{ij} \partial \epsilon_{kl}} \qquad \text{(II-12)}$$

This representation for the elastic constants as the second partial derivatives of the elastic energy with respect to the strain-tensor components leads naturally to the possibility of extending this result to include not only the elastic energy itself, but also the internal energy associated with the magnetic and magnetoelastic Hamiltonians. For the case of low-frequency elastic strain, this approach would lead to a simple method for the calculation of the magnetoelastic contributions to the elastic constants. Since such magnetoelastic contributions to the elastic constants of rare-earth materials are one of the most readily observable of the dynamic magnetoelastic phenomena, as seen in the following sections of this report, this point will be explored at some length below.

The kinetic elastic energy, in the classical limit, is given as the volume integral of the classical kinetic energy of each volume element of the lattice in the usual manner.

B. Method of Calculation

Because each type of rare-earth material presents a different physical configuration of the ions, leading to different detailed computational procedures for each of the many possible materials, detailed results of calculations based on the theoretical model described above are not give here. The general method of approach is described briefly, and specific results are given in the following sections, in which the experimental program and its results are described.

If the model described in the preceding section is adopted, the state of a crystalline specimen as a whole is described in terms of the thermodynamic functions which can be calculated on the basis of the model Hamiltonian. For example, in the calculation of the magnetoelastic contributions to the elastic constants, it is necessary to compute the internal energy, whose second partial derivatives are the conventionally defined adiabatic elastic constants. The calculation of a state function such as the internal energy, even in a simplified model such as that described here, requires rather complicated numerical computation even for paramagnetic or simple ferromagnetic materials. When periodic ordering is also considered, the computations become even more complicated. As a result, only a very few special cases have been worked out in any detail.

The general approach is the calculation of a quantum-mechanical density matrix operator. Then, the state variables may all be calculated by means of evaluating straightforward partition sums. Any partial derivatives which are then needed for the determination of elastic, magnetic, or magnetoelastic properties may usually be worked out numerically or, in some cases, analytically. The problem is complicated, however, in the case of the elastic constants and other second-order properties, requiring the calculation of second derivatives of state variables, in that the partition function or density matrix may vary in first order with respect to the strain of other variable of interest. Thus, the actual computation of magnetic and magnetoelastic properties may be rather difficult in many cases. Those specific results which have been worked out within the framework of this theoretical approach are described in the following sections.

It should be pointed out that the approach taken here is probably appropriate only when elastic waves whose wavelength is long compared to lattice spacings, and whose frequencies are low compared to natural relaxation rates, are considered. Otherwise, a coupled spinwave-phonon approach using second-quantization techniques

would be required. Such an approach was employed by Southern and Goodings[11], but, for the reasons mentioned above, and because of its greater complexity and difficulty of computation, this method was not employed in the theoretical interpretation of the experimental work described below.

III. EXPERIMENTAL OBSERVATIONS OF DYNAMIC MAGNETOELASTIC EFFECTS IN RARE-EARTH MATERIALS AND THEIR INTERPRETATION.

This section gives first, an overview of dynamic magnetoelastic effects in rare-earth materials. Then a description of work carried out in this program on magnetoelastic effects in terbium, erbium, and in various rare-earth-iron-group materials is given.

A. Dynamic Magnetoelastic Effects in Rare-Earth Materials: A Survey

The extremely strong magnetoelastic interactions found in many rare-earth materials lead to a number of interesting observable phenomena, the most striking of which is the so-called "giant" magnetostriction exhibited at low temperatures by the single crystals of the pure elements Tb, Dy, Ho, and Er[18]. Recently, Clark and Belson[21] have reported that a new class of compounds, the cubic Laves-phase materials, RFe_2, where R represents any of several rare-earth elements, also exhibit very large magnetostriction, even in polycrystalline specimens at room temperature. The static-equilibrium magnetostriction of the pure rare-earth elements is at present fairly well understood in terms of a theory due to Callen and Callen[7], who took into account both single-ion magnetoelastic interactions arising from the strain dependence of the the crystal-field anisotropy energy and two-ion magnetoelastic interactions arising from the strain dependence of the exchange interaction energy between pairs of ions. The experimental results of Clark, DeSavage, and Bozorth[22] on the static magnetostriction of single-crystal dysprosium are in particularly good agreement with the theory of Callen and Callen.

This report is concerned with magnetoelastic interactions in situations involving time-dependent elastic strains. Two principal areas are of interest here. The first is the effect of magnetoelastic interactions on the propagation of elastic waves in rare-earth materials. Both the velocity and the attenuation of elastic waves in magnetoelastic materials exhibit anomalous behavior compared to nonmagnetic materials, and the effect of the magnetoelastic interactions on the elastic-wave

velocity has been interpreted primarily in terms of the adiabatic elastic constants of rare-earth materials. These elastic constants are usually measured by measuring the velocities of elastic waves in the frequency range of several MHz along certain crystallographic directions, and, in the case of the rare-earth elements, the temperature dependences of the elastic constants exhibit behavior which is anomalous compared to that of most other materials. The temperature dependence of the elastic constants of several rare-earth elements is described in what follows, and an explanation of the magnetoelastic contributions to the elastic constants is given in terms of an extension of the theory of Callen and Callen to the domain of time-dependent lattice strain.

The second area of interest is the magnetoelastic generation of elastic waves. The phenomenon of magnetostriction has been used for many years in ultrasonic transducers, with many technological applications. When it was found, by Legvold, Alstad, and Rhyne[23] that single-crystal dysprosium and holmium both exhibit magnetostriction at low temperatures some 100 times greater than that of nickel and other iron-group materials, the interesting possibility was raised that such materials might lead to the development of highly efficient ultrasonic transducers, perhaps capable of operation at very high frequencies. Maley, Donoho, and Blackstead[24] reported ultrasonic elastic-wave generation in thin-film polycrystalline transducers of Gd, Dy, Ho, and Er at frequencies between 1,000 and 10,000 MHz, with efficiency somewhat greater than that observed in similar thin-film Ni transducers. The efficiency of the rare-earth transducers was not, however, as high as would have been expected from a simple comparison of the static magnetostriction of these rare-earth elements with that of nickel. This deficiency was attributed in part to the lack of purity of the films and to their polycrystalline nature. The rare-earth transducers also possessed the serious defect, from the standpoint of using them in practical applications, that they required low temperatures and high magnetic fields for their operation.

The recent discovery by Clark and Belson[21] that the intermetallic compound $TbFe_2$ exhibits very large static magnetostriction at room temperature in polycrystalline specimens suggested that this new material might avoid the difficulties mentioned above and lead to the possibility of the development of worthwhile new magnetostrictive transducers. Magnetostrictive ultrasonic generation was observed in thin films of this material by Donoho *et al*[25] at room temperature and at frequencies from 300 MHz to 1,500 MHz. The results which have been obtained to date on magnetostrictive generation in the pure rare-earth elements and in Tb-Fe films

are reviewed briefly in this section, and a more detailed account of the results obtained in this program on Tb-Fe compounds is given in a subsequent section.

1. Magnetoelastic Contributions to Elastic Constants

The temperature dependences of certain of the elastic constants of Tb, Ho, and Er are given in Figures 2 - 10. The elastic constarts of Tb and Ho were measured by Salama et al[26, 27], and those of Er have been measured by Hubbell et al[28]. In addition, the elastic constants of Gd have been measured by Long et al[29], and those of Dy have been measured by Rosen and Klimker[30]. However, only results obtained in the present program are shown in the figures. For a normal, nonmagnetoelastic, material, the elastic constants generally increase smoothly with decreasing temperature as the material becomes elastically "harder". As seen in Figs. 2-10, however, there are numerous departures from this normal behavior in the case of the rare-earth elements.

In the case of Tb, as the temperature is lowered, there is a paramagnetic-helimagnetic phase transition at T_N = 230 K and a helimagnetic-ferromagnetic transition at T_C = 219 K. At both of these transition temperatures the elastic constants of Tb exhibit anomalous behavior. The elastic constant c_{11}, for example, has cusp-like anomalies at these temperatures, whereas c_{33} exhibits even more pronounced anomalies, as does c_{66}. On the other hand, c_{44} undergoes only a change in slope at the second-order transition at T_N, while it exhibits a small cusp at the first order transition at T_C.

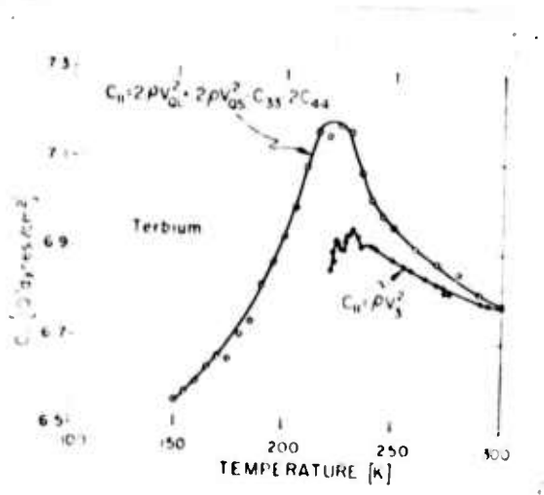

Fig. 2 Temperature dependence of c_{11} for single-crystal Tb.

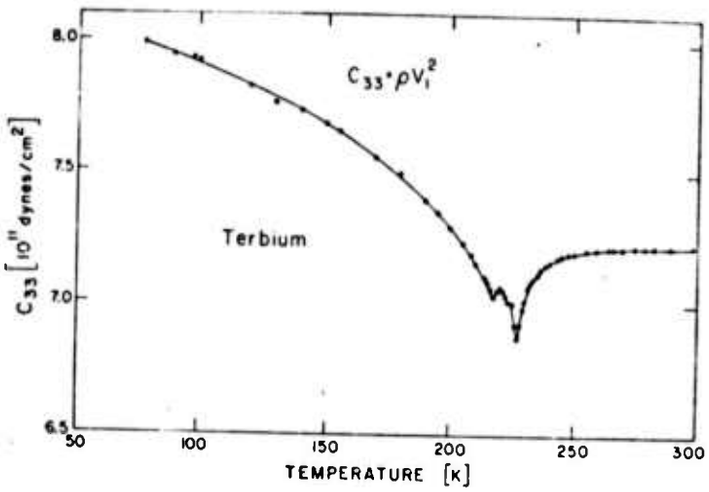

Fig. 3 Temperature dependence of c_{33} for single-crystal Tb.

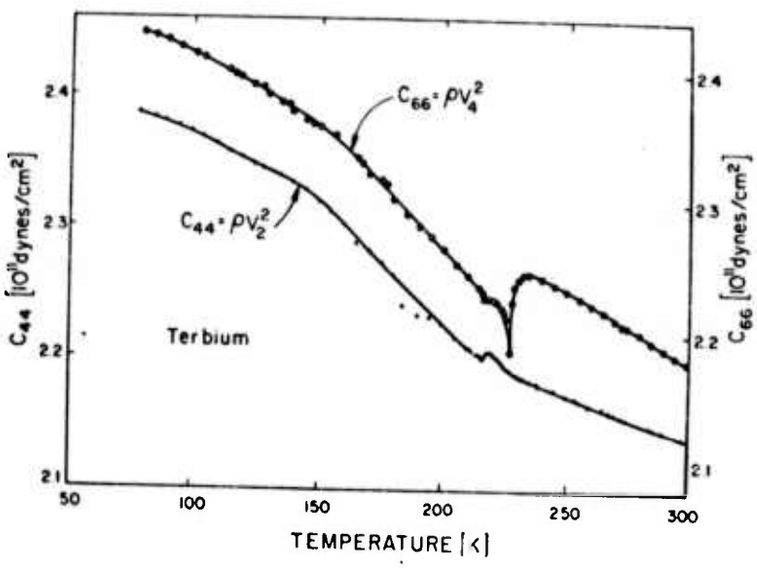

Fig. 4 Temperature dependences of c_{44} and c_{66} for single-crystal Tb.

For the elastic constants of Ho, the qualitative nature of the magnetoelastic contributions to the elastic constants is similar, as seen in Figs. 4-7. In this case, unfortunately, strong elastic-wave attenuation prevented measurements below approximately 80 K, and only the anomalies at the second-order paramagnetic-helimagnetic phase transition at T_N = 130 K can be seen. The first-order helimagnetic-ferromagnetic transition at T_C = 20 K could not be observed. In the case of Ho,

it can be seen that c_{11} undergoes only a change in slope at T_N, but that c_{33} exhibits a very large cusp-like anomaly at this temperature. Both c_{44} and c_{66} undergo only changes in slope at T_N.

The case of erbium is, in some ways, the most interesting of those discussed here. It is worthwhile to consider in some detail the magnetic ordering phases of Er, as shown in Fig. 11.

Fig. 5 Temperature dependence of c_{11} for single-crystal Ho.

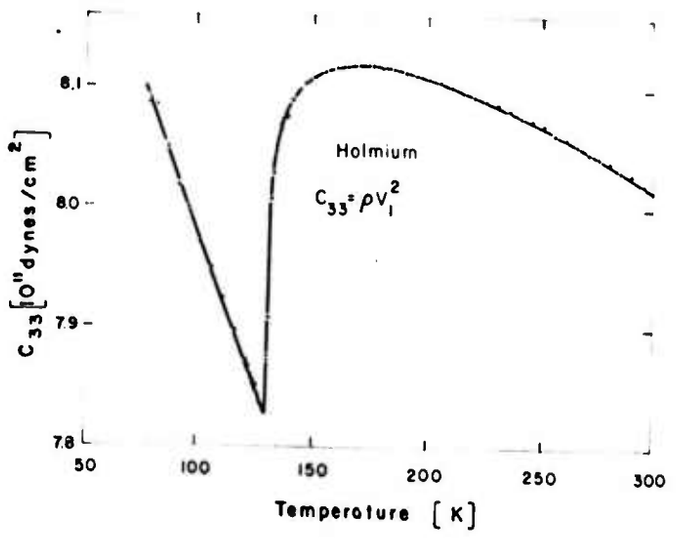

Fig. 6 Temperature dependence of c_{33} for single-crystal Ho.

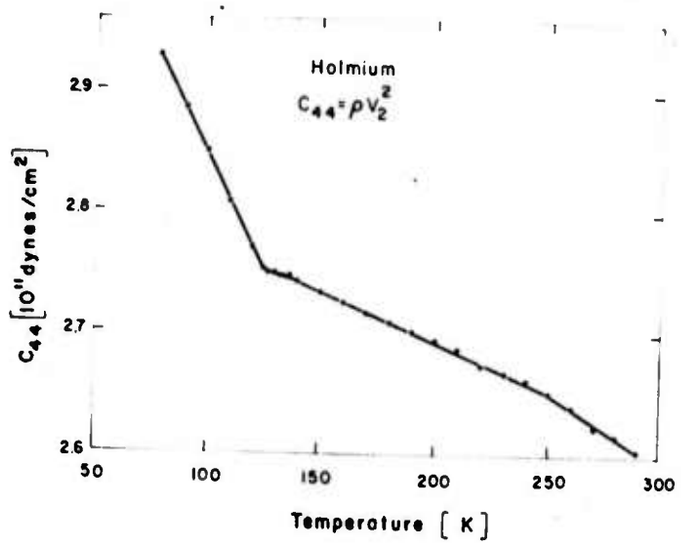

Fig. 7 Temperature dependence of c_{44} for single-crystal Ho.

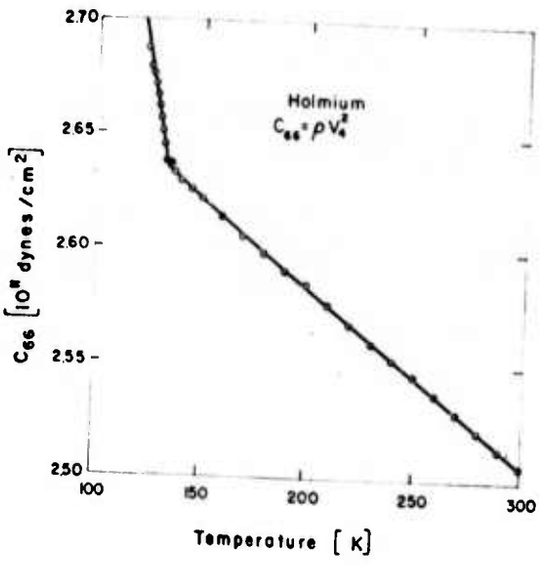

Fig. 8 Temperature dependence of c_{66} for single-crystal Ho.

Above T_N = 86 K, Er is paramagnetic, whereas for temperatures between T_Q = 52 K and T_N it is antiferromagnetic, with a sinusoidal modulation of the c-axis component of the magnetization of each basal-plane layer of ions. Between T_C = 20 K and T_Q the ordering is such that the c-axis component of the magnetization of each plane of ions exhibits a square-wave-like behavior in going from one plane to another, while the basal-plane component is helically ordered. Below T_C the ordering

is conically ferromagnetic, with a uniform c-axis component of the magnetization and a helical ordering of the basal-plane component of the magnetization.

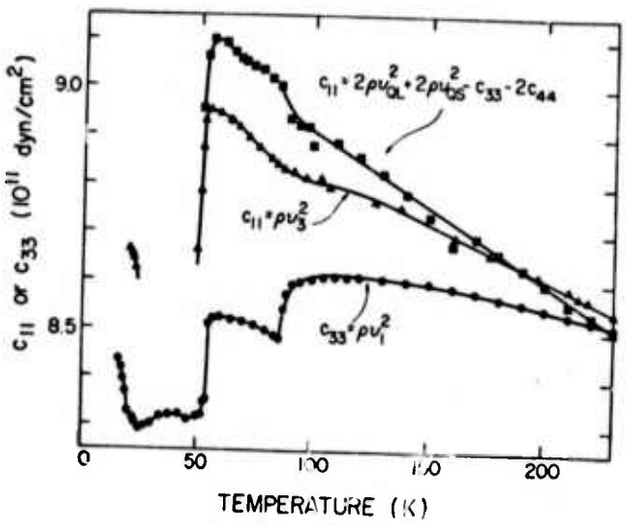

Fig. 9 Temperature dependences of c_{11} and c_{33} for single-crystal Er.

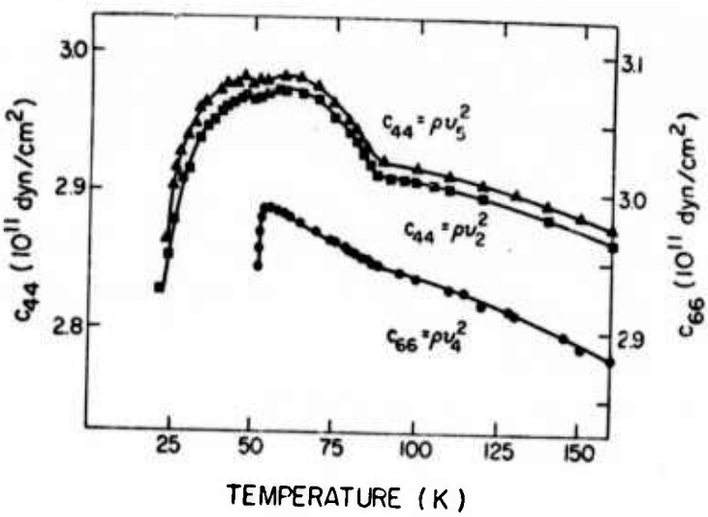

Fig. 10 Temperature dependences of c_{44} and c_{66} for single-crystal Er.

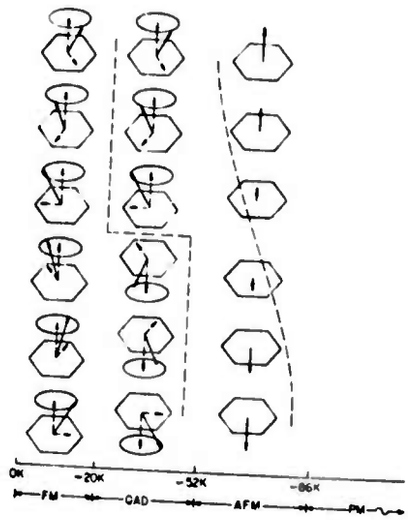

Fig. 11 Magnetic Ordering Phases of Single-Crystal Er.

It is obvious from a number of considerations that the transition at T_N is a second-order thermodynamic phase transition and that the transition at T_C is a first-order transition. The neutron-diffraction data of Cable et al[31] do not, however, permit any deduction to be made concerning the transition at T_Q If this transition were made abruptly at T_Q to the antiferromagnetic structure below this temperature as the temperature was lowered from the sinusoidal range above T_Q, then the transition would surely be a first-order transition. On the other hand, if the helically ordered component of basal-plane magnetization only develops gradually, starting from a zero amplitude at T_Q, with no discontinuity in the magnetization of the c-axis magnetization at this temperature, then the transition should be of second order. The behavior of the elastic constants at T_Q sheds some loght on the nature of this phase transition. In addition, useful information is also provided by the behavior of the elastic-wave attenuation shown in Figs. 12 and 13.

In the cases of all the rare-earth elements whose elastic constants have previously been measured, including Dy[30], for which the results are not shown here, the elastic constant c_{44} invariably undergoes a change in slope at a second-order transition and a cusp-like discontinuity at a first-order transition. From this observation, one would surmise that the transition at T_Q is, in fact, a second-order transition. The evidence from the elastic-wave attenuation shown in Figs. 12 and 13 supports this conclusion, since the shear-wave attenuation exhibits no peaks at T_N or T_Q, but it does undergo a sharp change at the first-order transition at T_C.

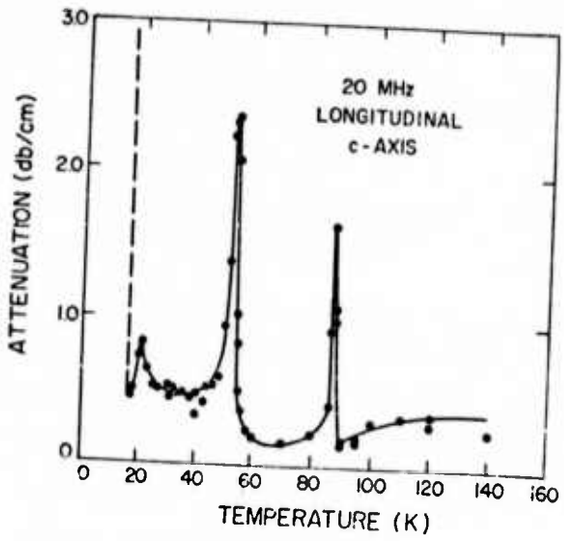

Fig. 12 Temperature dependence of longitudinal c-axis attenuation in Er.

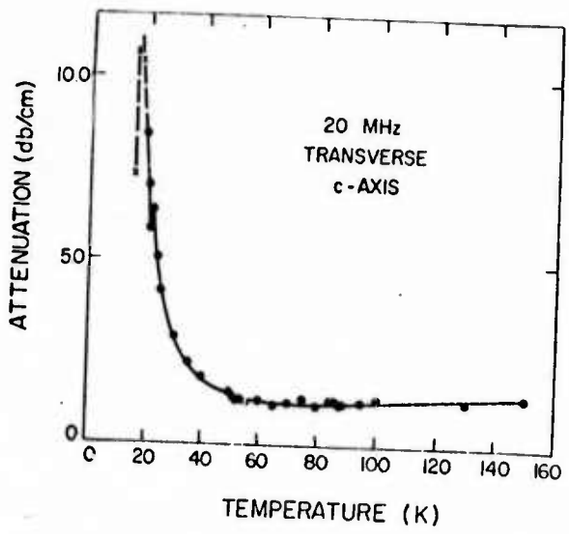

Fig. 13 Temperature dependence of shear c-axis attenuation in Er.

The elastic constants which are determined from measurements on the velocities of elastic waves are the adiabatic elastic constants, and they can be regarded, as discussed in a previous section of this report, as the second partial derivatives of the thermodynamic internal energy of the crystal with respect to the components of the lattice strain. In order to calculate the magnetoelastic contribution to the elastic constants, therefore, it is necessary to compute the dependence of the internal energy to second degree in the strain for the magnetic and magnetoelastic parts of the Hamiltonian which characterizes the state of the crystal. Such a calculation is difficult in a magnetically ordered material because of the difficulty arising in attempting to treat the exchange interactions. A certain degree of success has been obtained, however, in describing the behavior of the magnetoelastic contributions to the elastic constants of Gd by Freyne[10], utilizing a molecular-field approximation to treat the exchange interactions. A similar approach was followed by Hubbell *et al*[28] to explain the behavior of c_{33} in Er in the vicinity of the paramagnetic-antiferromagnetic phase transition at T_N = 86 K. These authors took account only of the single-ion magnetoelastic interaction defined in the previous section, and they used results obtained by Nagamiya[13] for the amplitude of the sinusoidally modulated c-axis magnetization below T_N in their calculation of the magnetic and magnetoelastic contributions to the internal energy. In this way, Hubbell *et al* were able to obtain a reasonably good fit to the behavior of c_{33} near T_N, as shown in Fig. 14.

The detailed computation of the temperature dependence of all the elastic constants remains a difficult problem, primarily because of the complexity of the magnetic-ordering phases of these materials. Southern and Goodings[11] have developed a theory of the magnetoelastic contributions to the elastic constants of the rare earths making use of a rotationally invariant approach not included in previous treatments of dynamic magnetoelastic interactions. Their approach, which also takes account of the quadratic nature of the conventional definition of finite lattice strain, was developed primarily to explain the dependence of the elastic constants on applied magnetic fields, and it should permit a more satisfactory approach to the problem of the temperature dependence of the elastic constants. An experiment motivated by the work of Southern and Goodings[11] on the field dependence of the elastic constants of paramagnetic Tb is described in a subsequent section of this report.

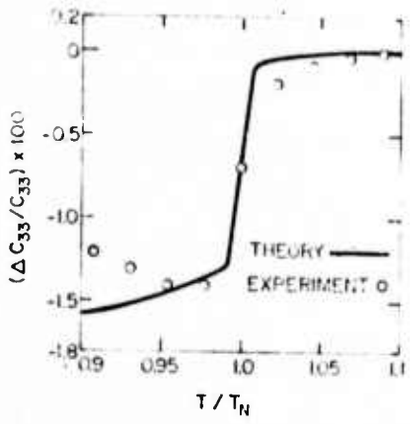

Fig. 14 Comparison of experimentally determined temperature dependence of c_{33} in Er near T_N = 86 K with theory using molecular-field approximation and single-ion magnetoelastic interaction.

2. Magnetostrictive Generation of Ultrasonic Waves

The magnetostrictive generation of high-frequency elastic waves in rare-earth materials was first reported by Maley, Blackstead, and Donoho[24], who observed strong magnetostrictive elastic-wave generation at frequencies in the range 1,000 to 10,000 MHz in films of 2-μm thickness of Gd, Dy, Ho, and Er vacuum evaporated onto substrate delay lines of quartz and sapphire. This work was extended by Donoho et al[25] to include Tb and the intermetallic compound $TbFe_2$. The films were placed in an rf cavity in a region of maximum rf magnetic field, with the rf field parallel to the film surface. A dc magnetic field up to 60 kOe could be applied at any direction with respect to the surface of the film. An rf pulse was applied to excite the magnetostrictive generation of the elastic waves, which then gave rise to a sequence of ultrasonic pulse echoes in the delay-line substrate. Typical results for the field dependence of the amplitude of elastic waves magnetostrictively generated in Dy and Tb are shown in Figs. 15 and 16.

Two important features of the magnetostrictive generation of ultrasonic waves in the pure rare earths are evident in Figs. 15 and 16. First, appreciable efficiency of generation occurs only in the presence of large applied fields; second, because the magnetic ordering temperatures of these materials are in the

cryogenic range, they can be used as transducers only at temperatures so low that their usefulness in practical applications is severely limited. Another somewhat disappointing feature of the magnetostrictive generation of elastic waves in pure rare-earth films is the fact that the maximum generation efficiency is not as great as might have been expected from the static magnetostriction. In this respect, the polycrystalline nature of the films used to study ultrasonic generation is probably responsible for the low efficiency.

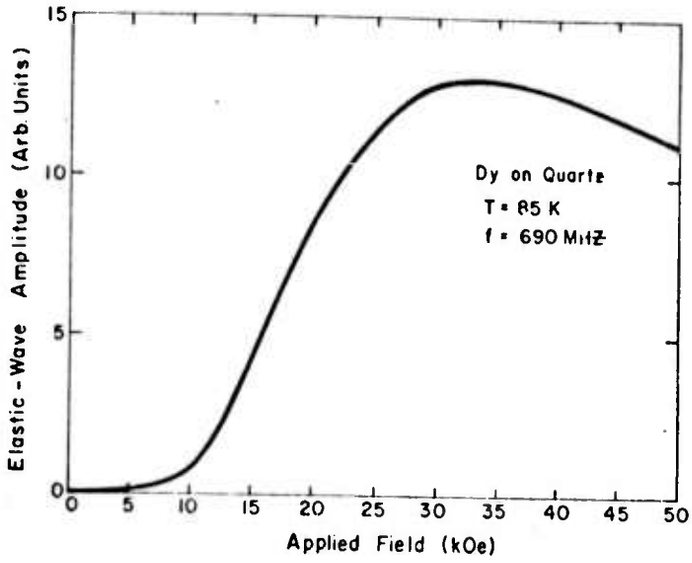

Fig. 15 Ultrasonic echc amplitude for Dy film on X-cut quartz substrate as a function of applied magnetic field perpendicular to plane of field.

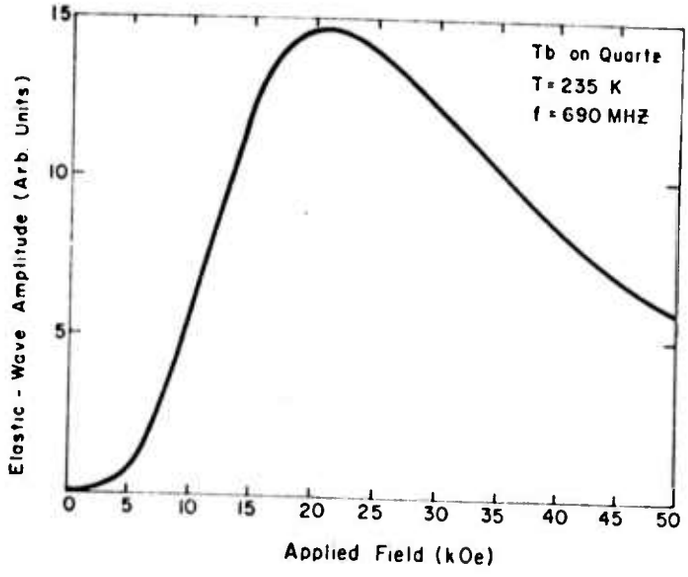

Fig. 16 Ultrasonic echo amplitude for Tb film on X-cut quartz substrate as function of applied field.

It is evident that, despite the enormous static magnetostriction exhibited by single crystals of the pure rare-earth elements at very low temperatures, these materials will not become useful as magnetostrictive transducers. Consequently, when Clark and Belson[21] reported their observation that the intermetallic compound $TbFe_2$ exhibits very large magnetostriction at room temperature in polycrystalline specimens, it appeared that this new material would probably be a much better candidate for the development of a good high-efficiency room-temperature ultrasonic transducer. Thin-film specimens of $TbFe_2$ were, therefore, deposited on delay-line substrates, and it was quickly demonstrated[25] that ultrasonic generation at room temperature and at high frequencies (700 MHz) was feasible with this material. A particularly interesting feature of the magnetostrictive ultrasonic generation in $TbFe_2$, however, and a totally unexpected feature, was the fact that thin films of this materials, unlike bulk specimens, exhibit a very strong coercive force and a very high degree of anisotropy, leading to a strong remanent magnetization perpendicular to the plane of the film. This strong remanence permits the generation of ultrasonic waves at high efficiency without the requirement of an applied magnetic field. The results obtained on Tb-Fe films of various compositions are given in more detail in a subsequent section of this report.

In conclusion, it has not yet been successfully demonstrated that rare-earth materials will compete with currently available ultrasonic transducer materials, but the compound $TbFe_2$ shows enough promise to warrant further study.

B. Magnetoelastic Coupling in Paramagnetic Terbium

As discussed above, the strong magnetoelastic interactions found in most rare-earth materials lead to significant magnetoelastic contributions to the elastic constants of these materials. The principal way in which these magnetoelastic contributions are manifested is in the anomalous temperature dependence of the elastic constants, particularly near magnetic phase transitions. Such anomalies have been observed in the cases of Gd[29], Dy[30], Tb[26], Ho[27], and Er[28], and, in some cases, they amount to anomalous deviations of the elastic constants of several per cent from what would be expected for a non-magnetoelastic material. Attempts to explain these magnetoelastic contributions to the elastic constants in terms of the fundamental magnetoelastic interactions of the rare-earth elements have, however, been only partially successful because of the difficulty encountered in calculating such thermodynamic functions as the internal energy near a phase transition

in a magnetically ordered material. Southern and Goodings[11] have, however, in a paper concerned with the general problem of the magnetoelastic contributions to the elastic properties of rare-earth materials, pointed out that these magnetoelastic contributions to the elastic constants would, perhaps, be significant even in the paramagnetic temperature range, where calculations may usually be made with greater confidence than in the magnetically ordered phases. In their approach to this problem, Southern and Goodings, basing their work in part on earlier work of Melcher[19] and Brown[20], developed a rotationally invariant theory of magnetoelastic interactions, and they took account of the nonlinear nature of finite strains to arrive at a simple result for rare-earth materials in the paramagnetic phase.

Motivated by the work of Southern and Goodings[11] in calculating the magnetoelastic contributions to the elastic constants c_{11} and c_{33} for rare-earth materials in the paramagnetic phase, an experiment was carried out on the dependence of these two elastic constants on temperature and on the value of an applied magnetic field for the case of paramagnetic terbium at temperatures from just above T_N = 229 K to approximately 300 K. The results of this experimental work are in at least partial agreement with the predictions of the theory of Southern and Goodings, and they permit an estimate of the values of certain of the fundamental single-ion and two-ion magnetoelastic coupling constants of terbium. The estimated coupling constants, however, exhibit an unexpected temperature dependence not accounted for by the theory. It is believed, however, that measurements over a greater temperature interval, using considerably larger applied magnetic field values, would probably lead to better agreement between the experimental results and the theory of Southern and Goodings. Such an extension of the work reported here is planned, and a similar experiment has been started for the case of paramagnetic dysprosium.

1. Theory

In this section, that part of the theory of Southern and Goodings[11] pertinent to the present discussion is outlined. These authors utilized both single-ion and two-ion magnetoelastic interactions, and they took account of the quadratic nature of the conventionally defined finite lattice-strain tensor. Since the present interest lies only in the elastic constants c_{11} and c_{33}, which are measured by observing the velocities of longitudinally polarized elastic waves propagated along the crystallographic a-, b-, or c-axes, the magnetoelastic

interaction Hamiltonian used by Southern and Goodings is truncated here to include the effects only of these longitudinal strains.

The single-ion Hamiltonian for the magnetoelastic interaction, subject to the truncation mentioned above, is given by

$$H_{me}^{I} = - M_{20}^{\alpha,1} \sum_i E^{\alpha,1} J_{20}(i) - M_{20}^{\alpha,2} \sum_i E^{\alpha,2} J_{20}(i) - M_{22}^{\gamma} \sum_i E_1^{\gamma} J_{22}^{+}(i), \qquad \text{(III-1)}$$

where the M-coefficients are the single-ion magnetoelastic coupling constants defined by Southern and Goodings, the E-components are the components of the finite-strain irreducible tensor, and the J-operators are the second-rank irreducible tensor angular-momentum operators defined in a previous section and in Appendix I. The index i is a label for each ion in the system. The two-ion magnetoelastic Hamiltonian is given by the following expression:

$$H_{me}^{II} = \sum_{i<j} H_{me}^{II}(i,j) \qquad \text{(III-2a)}$$

$$H_{me}^{II}(i,j) = -[D_{11ij}^{\alpha} E^{\alpha,1} + D_{21ij}^{\alpha} E^{\alpha,2}] \vec{J}_i \cdot \vec{J}_j$$

$$-[D_{12ij}^{\alpha} E^{\alpha,1} + D_{22ij}^{\alpha} E^{\alpha,2}] \frac{\sqrt{3}}{2} [J_i^z J_j^z - \frac{1}{3} \vec{J}_i \cdot \vec{J}_j]$$

$$- D_{ij}^{\gamma} E_1^{\gamma} [J_i^x J_j^x - J_i^y J_j^y] \qquad \text{(III-2b)}$$

In these equations, i and j refer to a particular pair of ions, and the D- coefficients are the two-ion coupling constants. The M- and D- coefficients are determined by the strain dependence of the magnetocrystalline anisotropy energy and the exchange energy, respectively.

Southern and Goodings recognized that in the paramagnetic phase all the second-degree angular-momentum operators appearing in both the single-ion and two-ion magnetoelastic Hamiltonians given above would, to a good approximation, contribute to the internal energy of the crystal to a degree proportional to the square of the reduced magnetization and, hence, in the paramagnetic phase, to the square of the applied magnetic field. Following Southern and Goodings, the following quantities can be defined:

$$b_1^{\alpha} = N M_{20}^{\alpha,1} J(J-1/2) \quad ; \quad b_2^{\alpha} = N M_{20}^{\alpha,2} J(J-1/2) \quad ;$$

$$b^{\gamma} = N M^{\gamma}_{22} J(J-1/2) \quad ; \quad d^{\gamma} = N \frac{J^2}{2} \sum_j D^{\gamma}_{ij} \quad ;$$

$$d^{\alpha}_{11} = N \frac{J^2}{2} \sum_j D^{\alpha}_{11ij} \quad ; \quad d^{\alpha}_{21} = N \frac{J^2}{2} \sum_j D^{\alpha}_{21ij} \quad ;$$

$$d^{\alpha}_{12} = N \frac{J^2}{2} \sum_j D^{\alpha}_{12ij} \quad ; \quad d^{\alpha}_{22} = N \frac{J^2}{2} \sum_j D^{\alpha}_{22ij} \quad ,$$

where N is the number of ions per unit volume. The following expression then corresponds to the one obtained by Southern and Goodings for the magnetoelastic contributions to c_{11} and c_{33} :

$$\Delta c_{33} = [\ (A + 2B) P_2(\cos\theta) + C + D\ ]\ F(T)\ H^2 \qquad \text{(III-3)}$$

$$\Delta c_{11} = [\ (A - B)\ P_2(\cos\theta) + C - D \pm E \sin^2\theta \cos 2\phi]\ F(T)\ H^2 \qquad \text{(III-4)}$$

In the above equations, $F(T) = [\ \chi_{\theta}(T)/M_o]^2$, where $\chi_{\theta}(T)$ is the anisotropic susceptibility and M_o is the satuaration magnetization. The angles, θ and ϕ, are the polar angles of the direction of the magnetic field with respect to the crystallographic c-axis and a-axis. In eq. (III-4) the plus sign is used when c_{11} is to be determined by measuring the elastic-wave velocity along the a-axis.

Thus, according to the calculations of Southern and Goodings, the changes in the two elastic constants of interest in an applied magnetic field should be proportional to the square of the value of the applied field and to the square of the magnetic susceptibility. The functions A through E, defined above, all functions of the fundamental magnetoelastic constants, should be reasonably constant throughout the paramagnetic temperature range. Examination of Eqs. (III-3) and (III-4) reveals that if the magnetoelastic changes in c_{11} and c_{33} can be measured accurately for any arbitrary direction of the applied field, then the constants A through E may all be determined if enough independent field directions are chosen for the measurements. The actual choice of directions is discussed in the following section.

2. Experimental Procedure

The single-crystal specimen of terbium used in this work was prepared by standard spark-erosion techniques, as described elsewhere[26]. For the measurement of c_{33}, 20-MHz longitudinally polarized elastic waves were propagated along the crystallographic c-axis, and for the measurement of c_{11} longitudinal waves of

the same frequency were propagated along the b-axis. The elastic constants were measured to a high degree of accuracy using a pulse-superposition spectrometer described elsewhere[26] to measure the velocities of the elastic waves. The temperature of the specimen was maintained at any desired value in the range of interest, 230 K to 300 K, by means of a continuous-flow cryostat and a temperature-control system of commercial design. The specimen was positioned in an electromagnet such that the field, with a maximum value of 18 kOe, could be directed along any desired crystallographic direction. In order to obtain a sufficient number of independent relations, employing eqs. (III-3) and (III-4), to permit a complete determination of all the quantities A, B, C, D, and E, three different field directions, along the a-, b-, and c-axes, were employed in the determination of the field dependences of the two elastic constants of interest. The field orientation used in the measurement of each elastic constant and the resulting relationship for the quantities A through E are given in Table I.

TABLE I

Elastic Constant	Field Direction	$\Delta c/F(T)H^2$
c_{33}	c-axis	$A + 2B + C + 2D$
c_{33}	a-axis	$-\frac{1}{2}(A + 2B) + C + 2D$
c_{11}	c-axis	$A - B + C - D$
c_{11}	a-axis	$-\frac{1}{2}(A - B) + C - D + E$
c_{11}	b-axis	$-\frac{1}{2}(A - B) + C - D - E$

For each of the orientations of the field, the field dependence of the elastic-wave velocities along the c-axis (leading to the determination of c_{33}) and along the b-axis (leading to the determination of c_{11}) were measured for temperatures from 230 K to 300 K. Although the orientation of the crystal was fairly accurately

determined through the use of X-ray techniques, the measured variation of the elastic-wave velocity with respect to the field direction could be used, as seen in Fig. 17, to confirm the orientation with the specimen in place inside the cryostat.

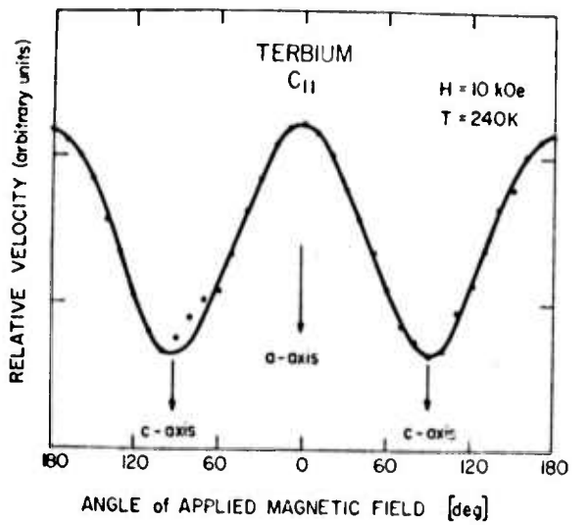

Fig. 17 Angular variation of b-axis longitudinal-wave velocity as field is rotated in a-c plane.

3. Results

The results of this work are depicted in Figs. 18 - 22, where the changes in the longitudinal elastic-wave velocities used to measure the elastic constants of interest are shown as functions of the square of the applied magnetic field for various temperatures. The straight lines shown on these figures, tangent to the actual experimentally determined curves at low fields, were used in the computations discussed below to represent slope $(\Delta v/v)/H^2$. It can be seen that the linear dependence of the relative change in velocity on the square of the applied field, as predicted by the theory of Southern and Goodings, is in reasonable agreement with the data for temperatures well above the Néel point. At the lower temperatures, near T_N, the experimental data at high fields deviate from the straight lines, undoubtedly because of the onset of saturation effects in the magnetization.

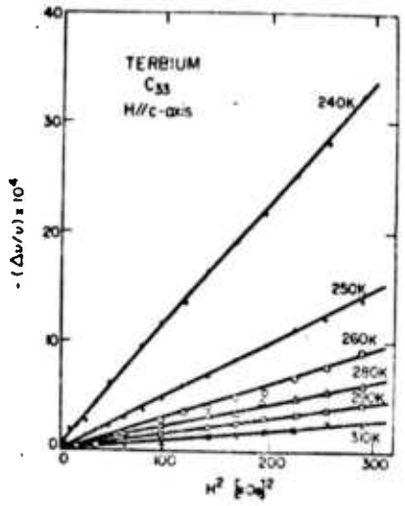

Fig. 18 Variation of c-axis longitudinal-wave velocity with H along c-axis.

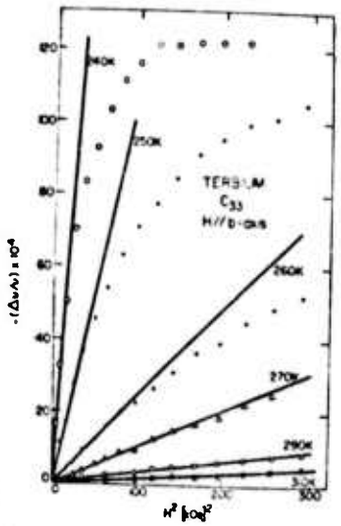

Fig. 19 Variation of c-axis longitudinal-wave velocity with H along b-axis.

The results shown in Figs. 18-22 were analyzed according to the theory of Southern and Goodings in the manner described above. The data of Hegland et al[32] were used for the susceptibility, and the data of Salama et al [26] for the elastic constants in zero magnetic field were employed in this analysis. A straightforward numerical computation was carried out, using the relations of table I toobtain values for the quantities A through E at each temperature. The values of the magnetoelastic coupling constants were then computed at temperatures from 240 K through 300 K, and the results are presented in Table II.

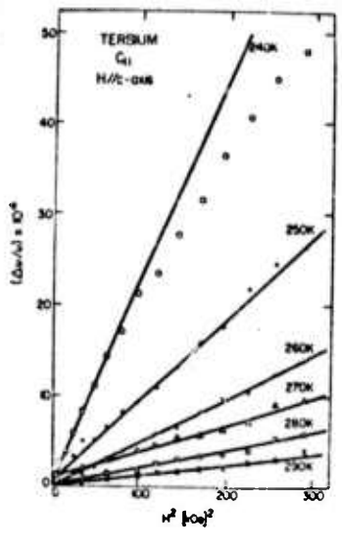

Fig. 20 Variation of b-axis longitudinal-wave velocity for H along c-axis.

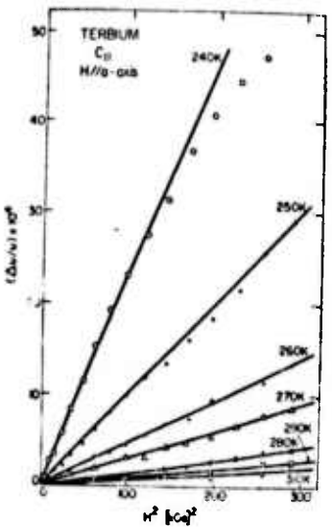

Fig. 21 Variation of b-axis longitudinal-wave velocity for H along a-axis.

It can be seen from Table II that there is a substantial, and unexpected, variation of the magnetoelastic constants with temperature over the range 240 K to 300 K. This variation of what were expected to be nearly temperature-independent constants over this limited range of temperatures is illustrated in Fig. 23, where the quantity $3b_2^{\gamma}/5 + d^{\gamma}$ is omitted for the sake of clarity.

The theory of both the single-ion and two-ion magnetoelastic interactions in rare-earth materials is based on the assumption that the crystal-field and exchange interactions are dependent upon the lattice strain[7]. This theory has

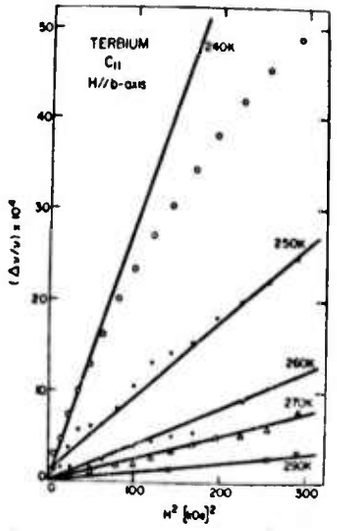

Fig. 22 Variation of b-axis longitudinal-wave velocity for H along b-axis.

TABLE II

T	$\frac{3}{5}b_1^\alpha + d_{12}^\alpha$	$\frac{3}{5}b_2^\alpha + d_{22}^\alpha$	d_{11}^α	d_{12}^α	$\frac{3}{5}b^\gamma + d^\gamma$
K	[		10^{11} erg/cm^3		]
240	- 8.87	6.09	0.34	20.58	- 0.40
250	- 5.38	3.54	0.22	13.13	0.22
260	-2.82	4.22	- 0.38	7.65	0.22
270	- 1.82	3.83	-0.34	6.25	0.30
280	- 1.32	4.12	- 0.19	5.76	- 0.21
290	- 0.78	2.60	- 0.01	4.76	- 0.23
300	- 0.37	1.84	0.17	4.04	0.37

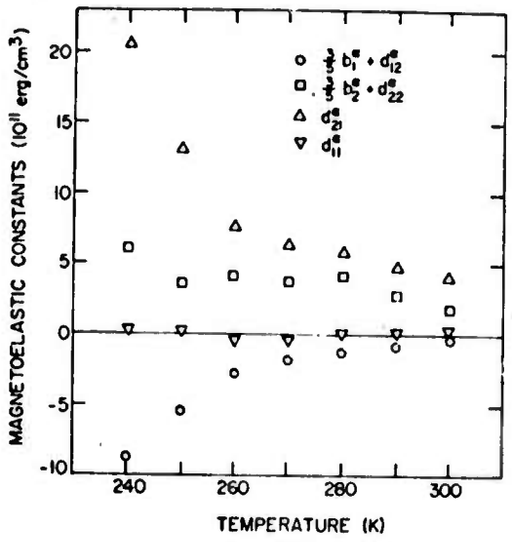

Fig. 23 Temperature dependence of the magnetoelastic coupling constants of single-crystal terbium.

been quite successful in explaining many of the observed features of the static magnetostriction of rare-earth materials[18]. One result of the comparison of the usual theory of the static magnetoelastic interactions with measurements of static magnetostriction is that the magnetoelastic coupling constants are, in fact, essentially constant over a very large temperature range, extending from temperatures in the liquid-helium range up to as high as room temperature. It is, therefore, rather surprising that such a large variation as that seen in Table II and Fig. 23 takes place over the limited temperature range from 240 K to 300 K. One would expect only a very small variation in both the M-constants and the D-constants over this range and, as a result, only a very small variation in the b- and d-quantities.

The theory of Southern and Goodings, however, upon which the analysis of the data obtained in the present work was based, does not appear to have neglected any important contributions to the field dependences of c_{11} and c_{33} in the paramagnetic state. The most probable reason for the large temperature dependence of the results given in Table II and Fig. 23 is the fact that the measurements reported here were all made over a range of temperatures fairly close to the ordering temperature, T_N = 229 K. The effects of short-range order near a phase transition always complicate the interpretation of the observed properties of any magnetic material, and it would appear that such is the case here, in the absence of any demonstrable deficiency in the theory of Southern and Goodings[11].

It would, therefore, be desirable to attempt to make similar measurements at somewhat higher temperatures, where the effects of the phase transition should be less important. Such measurements at higher temperatures would, however, be difficult without employing much larger values of the applied field than were available for the work reported here. It is anticipated that this work will be extended to higher temperatures in fields up to 55 kOe, and through such additional work it may be possible to measure the magnetoelastic coupling constants to greater accuracy than possible in the work reported here and to verify the theoretical predictions of Southern and Goodings in a more satisfactory manner.

C. Ultrasonic Generation in Terbium-Iron Thin Films

This section is concerned with the results of an investigation of magnetostrictive ultrasonic generation in thin films of terbium-iron compounds, particularly the cubic Laves-phase compound $TbFe_2$, which was recently found, by Clark and Belson[22], to exhibit very large static magnetostriction at room temperature in polycrystalline specimens. The work reported here was motivated by earlier studies on magnetostrictive ultrasonic generation in rare-earth materials[24,25].

In the cases of all the materials studied in the work reported here, namely $TbFe_2$, $TbFe_3$, TbFe, and $Tb_{0.3}Dy_{0.7}Fe_2$, filma of two-micrometer approximate thickness exhibited high for ultrasonic generation of shear elastic waves at frequencies in the vicinity of 680 MHz at room temperature. In the best cases, the magnetostrictive generation was about 100 times more efficient than that for piezoelectric longitudinal-wave generation in single-crystal X-cut quartz. A very interesting fe-ture of the $TbFe_2$ films was the discovery that they exhibited, under most cases of deposition onto quartz substrates, a strong uniaxial anisotropy, invariably with an easy axis of magnetization perpendicular to the plane of the film. A large remanent magnetization, amounting to some 80 per cent of the saturation value of the magnetization, was often observed, and coercive forces as high as 5 kOe were measured. As a result of this strong anisotropy, which was not at all expected, in view of the rather isotropic nature of bulk polycrystalline $TbFe_2$, strong ultrasonic generation was possible even in the absence of a biassing magnetic field. An interesting aspect of the existence of the anisotropy is the result that it is relatively simple to prepare a thin-film permanent magnet using $TbFe_2$, and it is possible that such magnets might find interesting applications in areas other than those considered here.

1. Experimental Technique

The specimen films were rapidly deposited from starting bulk material, prepared by ar-melting in an argon atmosphere, onto single-crystal X-cut quartz substrates which served as acoustic delay lines. Deposition was carried out at substrate temperatures in the vicinity of 300° C in a conventional vacuum system of st-rting pressure approximately 10^{-7} Torr. The evaporant was directly heated in a tungsten boat, with no apparent interaction with the boat, such as might be expected in the case of iron-group materials. The film thickness for which most measurements were made was approximately 2 μm, as determined by a commercial quartz-crystal thickness monitor. The $TbFe_2$ material used for most of this work was obtained from a commercial source. Some $TbFe_2$ and all the remaining materials were prepared in this laboratory, with the exception of the Tb-Dy-Fe ternary compound, which was kindly provided by A. E. Clark of the Naval Ordnance Laboratory.

The pulse spectrometer consisted of a commercial transmitter-receiver capable of operation over the frequency range 300-700 MHz, and it was equipped with a gated "boxcar" integrator to permit the detection of any selected ultrasonic echo and the accurate measurement of its amplitude. The specimen film was placed inside a stripline cavity, with the rf magnetic field parallel to the plane of the film. A dc magnetic field as large as 18 kG could be applied using a conventional electromeagnet. All measurements reported here were made at room temperature, in the vicinity of 295 K. The magnetization measurements, described below, which were carried out on the $TbFe_2$ films, were made using a Foner vibrating-sample magnetometer of high sensitivity, expecially constructed for this work.

2. Experimental Results

The results presented here on magnetostrictive ultrasonic generation in Tb-Fe materials were obtained at an ultrasonic frequency of 680-690 MHz at room temperature. Ultrasonic elastic waves were generated only with the applied dc magnetic field perpendicular to the plane of the film, and, in all cases, the waves were transversely polarized, with the plane of polarization parallel to the direction of the rf magnetic field. The determination of the plane of polarization was made from an examination of the shear-wave modes propagating in the quartz delay-line substrate. The substrate was normally oriented in the cavity such that the faster of the two shear-wave modes was used to observe the generation and detec-

of the elastic waves. In the figures which follow, the dc magnetic field was swept from zero up to a maximum value of 18 kOe, starting in the direction in which a field was last previously applied. It was then swept back through zero and all the way to 18 kOe in the opposite direction, returning finally to zero. Arrows on the figures indicate this sequence.

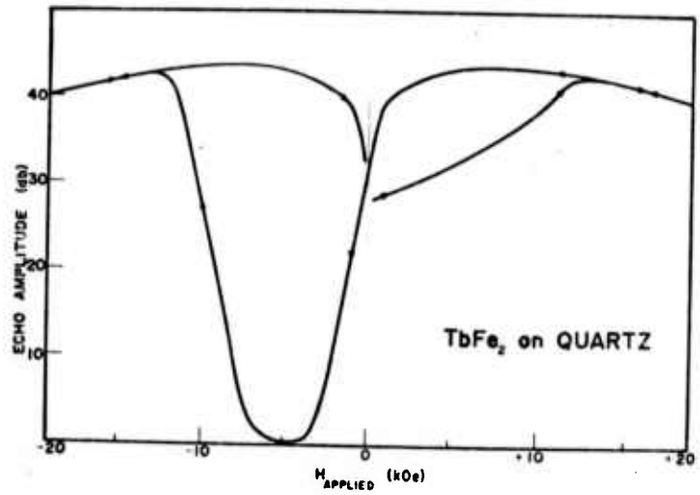

Fig.24 Ultrasonic echo amplitude as a function of applied magnetic field; $TbFe_2$ film on quartz substrate.

The field dependence of magnetostrictive ultrasonic generation in $TbFe_2$ films is shown in Fig. 24. This material was selected as the initial substance to be studied because of its large static magnetostriction at room temperature[21]. It exhibits ultrasonic generation efficiencies much higher than that of any other magnetostrictive materials which has been reported[24,25]. The generation efficiency for shear elastic waves at room temperature and a frequency of 680 MHz was typically 100 times that observed for longitudinal-wave piezoelectric generation in single-crystal quartz under the same conditions. The large hysteresis shown in Fig. 1 was, however, totally unexpected, since it implies a coercive force of the order of 4 kOe for these thin films. Although Clark et al[33] have shown that $TbFe_2$ does possess a large magnetic anisotropy, bulk specimens of this material do not exhibit any appreciable hysteresis nor do they possess a large coercive force.

A vibrating-sample magnetometer was used to measure the magnetization of the $TbFe_2$ films used in this work and to compare this magnetization with that of the

bulk material utilized for the preparation of the films. The results of these measurements are shown in Figs. 25 and 26.

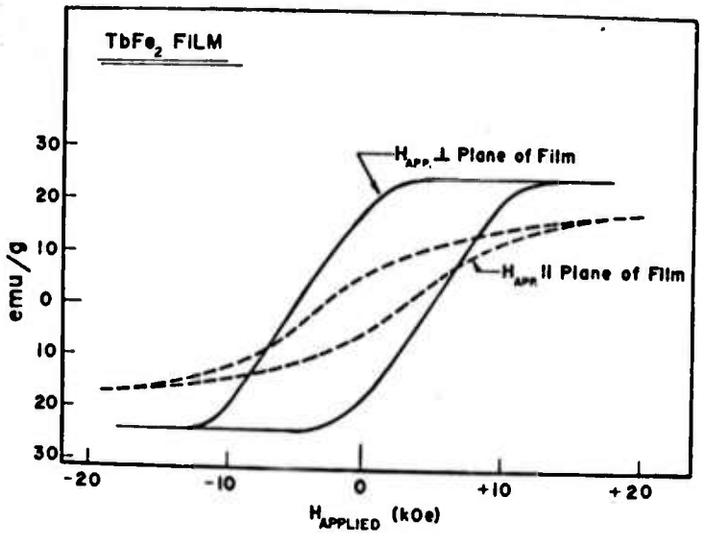

Fig. 25 Magnetization of $TbFe_2$ Thin films vs applied magnetic field.

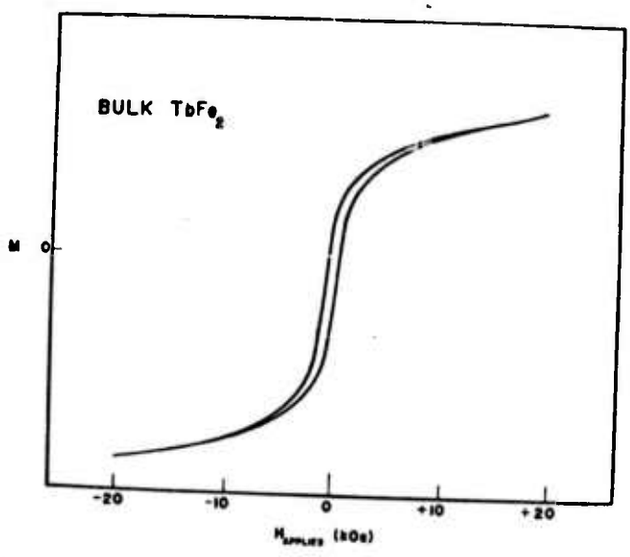

Fig. 26 Magnetization of bulk polycrystalline $TbFe_2$ vs applied magnetic field.

The magnetic anisotropy of the films is apparent in Fig. 25. For the case in which the field is applied perpendicular to the plane of the film, the coercive force is approximately 5 kOe, and saturation is apparently complete at a field of the order of 10-12 kOe. For the case in which the applied field is parallel to

the plane of the film, the coercive force is only of the order of 3 kOe, and saturation is not reached even for fields of the order of 20 kOe. By contrast, the specimen of bulk $TbFe_2$, although unsaturated at 20 kOe, exhibits little hysteresis, and it has no preferred anisotropy axis. Clark[34] has reported the development of high coercive forces in sputtered amorphous films of $TbFe_2$ after annealing in a strong magnetic field at temperatures above 300° C. The source of this strong anisotropy, with easy axis perpendicular to the plane of the film is not understood at this time, but it is undoubtedly due to at least some appreciable degree of crystallographic ordering. The anisotropy does, however, yield the fortunate result that a $TbFe_2$ film will remain strongly magnetized in the absence of an applied magnetic field, after first being magnetized to saturation. As a consequence, it is capable of efficient ultrasonic generation with no bias magnetic field. The magnetization data of Fig. 25 were used to plot the ultrasonic generation amplitude of Fig. 24 as a function of specimen magnetization, rather than applied field, with the result shown in Fig. 27. Here, it can be seen that the ultrasonic amplitude, in decibels, is nearly linearly dependent upon the specimen magnetization, a result predicted to some extent by the simple theoretical model of ultrasonic generation presented below.

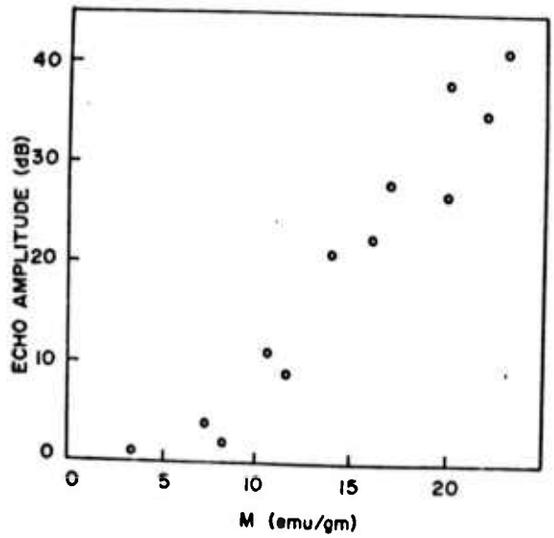

Fig. 27 Ultrasonic echo amplitude as a function of film magnetization; $TbFe_2$.

The ternary compound $Tb_{0.3}Dy_{0.7}Fe_2$ was also investigated, since Clark and Belson[21] had found that this material also exhibits large magnetostriction, but

that its anisotropy is much smaller than that of $TbFe_2$. Ultrasonic generation in thin films of this material is shown in Fig. 28, where it can be seen that there is almost no hysteresis. The maximum efficiency of generation in this case was comparable to that of $TbFe_2$. The compound $TbFe_3$ was also investigated, with the results shown in Fig. 29. Although there was substantial hysteresis, there was no remanent ultrasonic generation, and the peak efficiency was much smaller than that of $TbFe_2$.

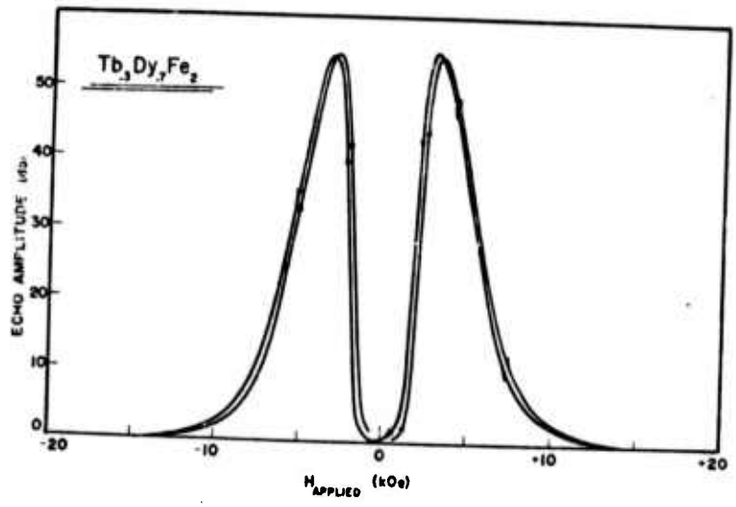

Fig. 28 Ultrasonic echo amplitude vs field for $Tb_{0.3}Dy_{0.7}Fe_2$ films.

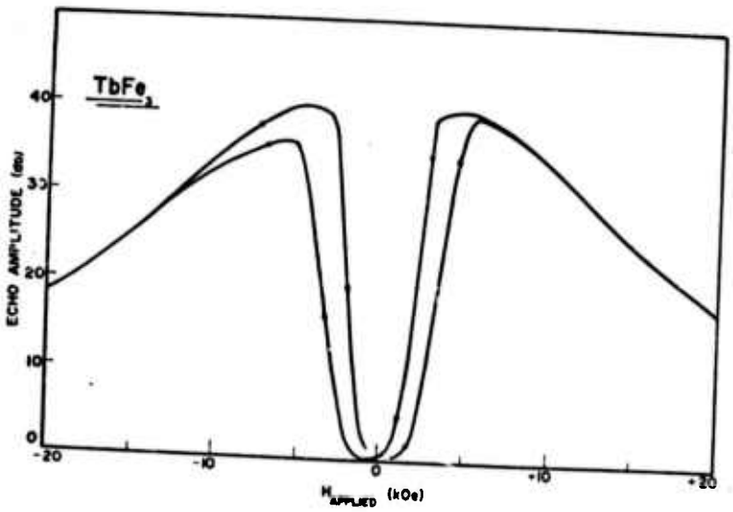

Fig 29 Ultrasonic echo amplitude vs field for $TbFe_3$ films.

3. Simplified Theory of Ultrasonic Elastic-Wave Generation

A simplified version of the theoretical model of Section II is employed here for the calculation of magnetostrictive ultrasonic generation of shear elastic waves in rare-earth materials. It should be pointed out that, in addition to the simplifying assumptions discussed in Section II, it is also assumed here, for the sake of avoiding unnecessary complexity, that the rare-earth ions are arranged in a simple ferromagnetic array, with every ion equivalent to all the others. Furthermore, for the present purpose, only the single-ion magnetoelastic interaction is taken into account. Only a qualitative understanding of the dependence of the ultrasonic generation amplitude on specimen magnetization is sought at this time.

It is assumed that the shear elastic waves propagate along the z-axis with polarization in the x-y plane in an isotropic medium. A dc magnetic field is applied along the z-direction, and a much smaller rf magnetic field is applied along the x direction at a frequency ω. If the particle displacement in the medium due to the elastic wave is denoted by $u(z,t)$ for the x-component and by $v(z,t)$ for the y-component, with corresponding shear strain $e_4 = \partial v/\partial z$ and $e_5 = \partial u/\partial z$, then the single-ion magnetoelastic Hamiltonian per ion may be written

$$H_{me} = B[\, e_4(J_yJ_z + J_zJ_y) + e_5(J_xJ_z + J_zJ_x)\,] \quad , \qquad \text{(III-5)}$$

where B is a magnetoelastic coupling constant, and the J_i are the components of the angular-momentum operator of the rare-earth ion. The purely magnetic Hamiltonian, neglecting anisotropy energy and assuming a molecular-field approximation for the exchange interaction, may be written (per ion)

$$H_m = g\,\mu_B[H_{rf}J_x + (H_o + H_e)\,J_z] \quad , \qquad \text{(III-6)}$$

where H_{rf} is the time-dependent applied rf magnetic field along the x-axis, and H_o is the applied dc magnetic field along the z-axis. The field H_e is the effective molecular field, which, for a simple, uniformly magnetized, ferromagnet, can be expressed as $H_e = \Gamma M_o \sigma$, where M_o is the saturation magnetization, Γ is a molecular-field constant, and σ is the reduced magnetization, M/M_o. To second order in perturbation theory, the internal energy associated with H_{me} can be expressed in the following way:

$$U_{me} = B\, e_5 \langle J_{20} \rangle H_{rf}/(H_o + H_e) \quad . \qquad \text{(III-7)}$$

In this expression, the operator J_{20} is defined as $3J_z^2 - J(J+1)$, and its thermal-equilibrium expectation value is given, from the work of Callen and Callen[7], as

$$\langle J_{20} \rangle = J(2J-1) I_{5/2}(W)/I_{1/2}(W) \quad , \qquad \text{(III-8)}$$

where W represents the inverse Langevin function of the reduced magnetization.

Now, if U_{me} is regarded as a strain- and field-dependent contribution to the internal energy, to be added to the normal elastic energy density, then the following wave equation for shear elastic waves propagating along the z-axis and polarized along the x-axis (parallel to the rf magnetic field) may be derived by standard techniques:

$$\rho \frac{\partial^2 u}{\partial t^2} = c_{44} \frac{\partial^2 u}{\partial z^2} + [NB\langle J_{20} \rangle/(H_o + H_e)] \frac{\partial}{\partial z} H_{rf} \quad . \qquad \text{(III-9)}$$

In the above expression, ρ is the density of the material, and c_{44} is a normal elastic constant. The second term on the right-hand side of the wave equation represents an inhomogeneous driving term in the wave equation which is responsibel for the generation of the elastic waves. The z-dependence of H_{rf} arises, of course, from the finite skin depth of the metallic specimen. Without going into the details of the solution of the wave equation, it can be seen that the amplitude of any elastic waves excited by the presence of the driving term will be proportional to the bracketed part of that term. Since H_e is normally much greater than H_o, the magnitude of the driving term in the wave equation will be proportional to $\langle J_{20} \rangle / \sigma$. A plot of this quantity is given in Fig. 30, where it can be seen that the predicted amplitude of the magnetostrictively generated elastic waves is expected to vary almost linearly with the specimen magnetization. Of course, the fact that the observed generation amplitude shown in Fig. 27 varies linearly as the specimen magnetization represents a somewhat different effect, being due to the rotation of domains into the direction of the applied field.

It should, of course, be recognized that the present treatment is simplified

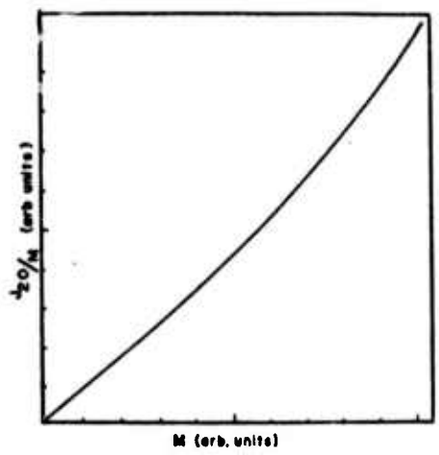

Fig. 30 Plot of $\langle J_{20} \rangle / M$ vs M.

to the point at which much detail would be lost. For example, any possibility of magnetic resonance has been excluded from the formulation given here, and this would seem to be required to account for the resonant-like behavior of the Tb-Dy-Fe compound shown in Fig. 28 . However, the experimental result that the polarization of the elastic waves generated magnetostrictively is parallel to the rf field is correctly predicted by this simplified treatment, and it might be expected that a fuller treatment, eliminating some of the large number of simplifying assumptions employed here, would lead to a reasonably good agreement between experimental results and theoretical predictions.

D. Magnetoelastic Effects in Erbium

As noted on numerous occasions in the preceding sections of this report, the very strong magnetoelastic interactions found in the heavy rare-earth elements give rise to a number of interesting phenomena. The subject of this section is a description of two dynamic magnetoelastic effects observed in the course of studies of the general characteristics of elastic-wave propagation in single-crystal erbium. Erbium is the first of the rare-earth series of elements all of whose ordered magnetic phases include ordered c-axis components of the magnetization. For this reason, it is possible to observe the phenomenon of circular magnetoacoustic birefringence in erbium, and this section reports on the observation of this effect. It also occurs that the dependence of longitudinal elastic-wave velocities on the value of an applied magnetic field is quite large, and this section reports on this effect, manifested as a very large dependence of the elastic constant c_{33} on the strenght of the applied field.

Specifically, the work described in this section concerns the following two magnetoelastic effects. The first is the anomalous temperature dependence of the elastic constant c_{33}, which undergoes a step-like decrease at the magnetic phase transitions rather than the cusp-like behavior exhibited by other elements[26-30]. Furthermore, the application of a magnetic field of 30-50 kG produces a very large decrease in the value of c_{33} in the vicinity of T_N (86 K). This large decrease, amounting to approximately 9 per cent, is much larger than any of the zero-field elastic-constant anomalies which have been reported. The second effect reported here is the observation of a large circular birefringence for elastic shear waves propagating along the c-axis of Er. At a temperature of 40 K in an applied c-axis field of 15 kG, this effect leads to a rotation of the plane of polarization of

approximately 0.65 rad/cm at a frequency of 20 MHz. An attempt has been made to explain the results given here in terms of the theoretical model of Section II of this report. The complicated magnetic structures of erbium make detailed calculation difficult, but some degree of qualitative agreement between theory and experiment has been achieved.

1. Experimental Technique

The single-crystal erbium specimens used in this work were prepared by standard spark-erosion techniques, with flat and parallel end surfaces perpendicular to the c-axis. The length along the c-axis was approximately [illegible]m. For the measurement of c_{33}, the pulse-superposition method was used to determine the elastic-wave velocity to high precision. For the birefringence measurements, a Matec, Inc. pulsed transmitter-receiver was employed to permit the measurement of the amplitude of a single ultrasonic echo. The ultrasonic frequency was 20 MHz for both types of measurement. For the measurement of c_{33} longitudinally polarized waves were employed, whereas for the observation of the birefringence transversely polarized waves were used. In the case of circular birefringence, which leads to a rotation of the plane of polarization of a linearly transversely polarized wave as it propagates, this rotation led to an oscillatory dependence of the detected echo amplitude as the applied magnetic field was varied, causing the rotation per unit length to change. An example of this oscillatory behavior is shown in Fig. 31. For the measurement of c_{33} and its dependence on applied fields, a superconducting solenoid capable of fields up to 60 kG was employed. (For the birefringence measurements, a conventional iron electromagnet capable of fields up to 18 kG was used.) For all measurements the specimen temperature was controlled within .05 K of the desired temperature through the use of a continuous-flow cryostat and conventional sensor-heater-feedback control system.

2. Circular Magnetoacoustic Birefringence

For the observation of circular birefringence, it is necessary that the elastic waves propagate along a crystallographic direction for which the two shear modes are normally degenerate in the absence of the magnetoelastic interactions. It is also necessary that there be a component of the magnetization, either spontaneous or induced, along the axis of propagation. Erbium is the only

readily available rare-earth element for which these requirements can be conveniently met, in that all of its magnetic ordering phases (discussed in Section II, Part A) involve ordered magnetization components along the c-axis. The c-axis is, of course, the only axis in a hexagonal crystal for which the two shear modes are degenerate. Figures 31 and 32 show some of the results obtained in the attempt to measure circular birefringence in single-crystal erbium.

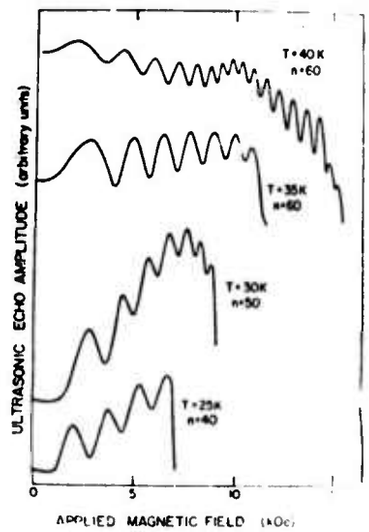

Fig. 31 Oscillations in the amplitude of the $n^{\underline{th}}$ shear-wave echo propagating along the c-axis of single-crystal Er.

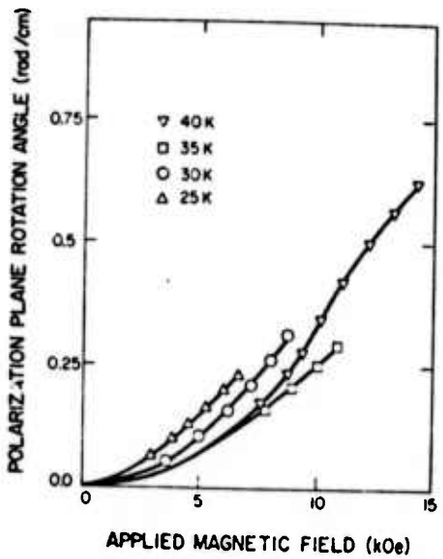

Fig. 32 Rotation of the plane of polarization of shear waves propagating along the c-axis in single-crystal erbium.

Fig. 31 shows the oscillatory behavior of the echo amplitude as a function of the applied field for several temperatures. The maxima of the oscillations occur when the rotation of the plane of polarization is an integral multiple of π, and the minima occur for odd half-integral multiples of π. From the data of Fig. 31, the curves of Fig. 32 were derived, giving the rotation per unit length of travel along the c-axis as a function of applied field for several temperatures in the so-called quasi antiphase domain region of erbium.

The observed rotation of the plane of polarization for shear waves in erbium could only be measured for temperatures in this ordering range because fields only as high as 18 kG were available for these measurements. Higher fields are necessary to produce a substantial c-axis net magnetization component at higher temperatures. As a result, the analysis of the results is somewhat more complicated than would be the case of measurements in, for example, the paramagnetic temperature range. Nevertheless, the theoretical approach described in Section II has been employed, again in a very simplified form, for the interpretation of the birefringence results in terms of the fundamental magnetoelastic interactions. An estimate for the shear single-ion magnetoelastic coupling constant $B^{\varepsilon,2}$ of 100 K per ion has been made, and this value is somewhat larger than the value for $B_2^{\alpha,2}$ of 20 K per ion which can be estimated from the static magnetostriction results of Rhyne and Legvold[35]. An improved agreement between theory and experiment can probably be obtained when measurements at higher temperatures are carried out.

3. Temperature Dependence of c_{33} for Erbium

The temperature dependence of c_{33} both in the absence of an applied magnetic field and in a field of 30 kG along the c-axis is shown in Fig. 33. The principal behavior in zero field is the step-like behavior at the Néel point, 86 K and at the lower phase transition at 52 K. The magnitude of the step at T_N is well understood, as discussed in Section III, Part A, where good agreement between theory and experiment was found when the magnitude of this step was calculated. The application of a field less than that required to induce a transition from the sinusoidally modulated c-axis ordered magnetization to ferromagnetic alignment has little effect on c_{33}, but above the threshold for this field-induced AFM-FM transition, the field gives rise to a very large decrease in the value of c_{33}. Because the state of the magnetization below T_N is not

very well understood, it is difficult in this case to calculate the magnitude of the change in c_{33} due to the presence of the field. If, however, the ferromagnetic alignment is assumed to be complete just below T_N in the presence of the large applied field, the theory discussed above leads to a predicted decrease in c_{33} of 12 per cent, only slightly larger than the observed decrease, if the magneto-elastic single-ion coupling constants deduced from the results of Rhyne and Legvold[35] are used in the theory, The other elastic constants of erbium, which also exhibit significant zero-field anomalies, are only slightly affected by the application of magnetic fields up to 55 kG either parallel to or perpendicular to the c-axis.

E. Holographic Interferometric Measurement of Magnetostriction in Rare-Earth-Iron Compounds

This section reports the results of the application of the relatively new technique of holographic interferometry to the measurement of the static magnetostriction of small single-crystal specimens of the very interesting cubic Laves-phase rare-earth-iron compounds such as $TbFe_2$. As previously mentioned, $TbFe_2$ exhibits very large magnetostriction in polycrystalline form at room temperature[21], and it also possesses a very large magnetic anisotropy[36], although no single-crystal anisotropy measurements have been reported. In the research program described here, we have been successful in growing small single-crystal specimens of two RFe_2 materials, namely $ErFe_2$ and a ternary compound, $Er_{0.314}Tb_{0.686}Fe_2$. Although these crystals were too small to permit the usual strain-gauge type of measurement of the magnetostriction, it was possible, using the technique of holographic interferometry, to measure the magnetostriction along various crystallographic directions for these materials, and, in conjunction, measurements of the magnetization were also made.

1. Crystal Growth

The crystals employed in this work were grown by electron-beam zone refining of polycrystalline material which had been previously arc melted from the appropriate proportions of high-purity specimens of the constituent components. In general, it was not possible to obtain single-crystal specimens with any degree of repeatability, and the results presented here were obtained

with what were essentially randomly and accidentally grown small single-crystal grains extracted from a larger polycrystalline mass. Because of the peritectic behavior of most rare-earth-iron compounds, it will undoubtedly be difficult to obtain large single-crystal specimens grown under tightly controlled conditions, and so it was felt that it would be worthwhile to carry out several types of experimental measurement before attempting to grow better crystals. The details of the crystal-growing procedure are given elsewhere[37].

Because the compound $ErFe_2$ appeared to be most appropriate for the growth of single crystals, this material was chosen initially as the subject of this investigation. However, the first lot of supposedly pure polycrystalline erbium which was used in the preparation of the polycrystalline $ErFe_2$ actually contained a large percentage of terbium. As a result, the small single-crystal specimen which was obtained from this material was, in fact, a Tb-Er-Fe compound having, apparently, the same cubic Laves-phase structure as $TbFe_2$ or $ErFe_2$. The composition of this specimen was determined by the technique of electron-stimulated X-ray fluorescence, using an electron microprobe apparatus. The composition of the crystal actually used for magnetostriction and magnetization measurements was $Er_{0.314}Tb_{0.686}Fe_2$. The starting Er-Tb mixture did not contain nearly as high a proportion of Tb as did the single-crystal specimen, but it may be that the observed Tb-Er ratio in the final crystal is the result of some degree of selectivity in the actual crystal-growth process. A second lot of pure erbium was used in the preparation of a second single-crystal specimen, and its X-ray fluorescence analysis indicated that it was essentially pure $ErFe_2$. Both crystals were irregularly shaped, with linear dimensiona ranging from one to four millimeters.

2. Experimental Technique for Holographic Measurement of Magnetostriction

Because it had been anticipated that only very small crystals of RFe_2 compounds would be available, making the use of conventional methods for the measurement of magnetostriction difficult, if not impossible, a system was developed to permit the measurement of small deformations of small, irregularly shaped, bodies using the method of real-time holographic interferometry. Briefly, the method, which is described in considerable detail elsewhere[37], may be described as follows. A hologram is ofrmed of the object whose deformation is to be investigated, using coherent light from and argon-ion laser. The hologram is then

subjected to the same light source as that used in its original formation in such a way that the holographically reconstructed three-dimensional virtual image of the object coincides with the object itself. Now, when the object is displaced or deformed in any way, light reflected from its surface witll set up an interference pattern with light from the holographically reconstructed image of the original undeformed object. By careful measurements on the positions of the fringes which can be seen as a result of the interference pattern, it is possible to analyze all components of both the displacement and the strain of the object.

In the present application, the object to be studied with holographic interferometry is the magnetostrictive RFe_2 single-crystal specimen, which is located between the poles of an electromagnet. A hologram is first formed in the absence of an applied magnetic field, and its reconstructed image is superimposed upon the object, resulting in a fringeless interference pattern. The magnetic field is then increased, giving rise to magnetostrictive deformation of the RFe_2 crystal and producing a pattern of light and dark interference fringes. Analysis of the positions of these fringes then permits a complete determination of all the modes of magnetostrictive strain in the specimen. The details of the analysis are quite complicated, and they are given in great detail elsewhere[37].

Measurements were also made on the specimen magnetization using a conventional Foner vibrating-sample magnetometer constructed in this laboratory.

3. Experimental Results

The static room-temperature magnetostriction of the two single-crystal specimens along various crystallographic axes are depicted on Figs. 34 and 35. The magnetization data are shown in Figs. 36 and 37. Although these data are only preliminary, they reveal quite interesting features. Consider first the case of $ErFe_2$. The magnetization curves are quite similar to those given by Clark and Belson[36], as expected, showing a high degree of saturation for magnetization along the [111] direction both in the case of the magnetization and the magnetostriction. The magnetostriction is not very large, amounting to at most a few hundred parts per million, although even this value is considerably larger than that of most iron-group materials. For the Er-Tb-Fe ternary crystal, again the [111] direction is the easy axis, but the anisotropy is apparently much stronger. What is really interesting is the magnitude of the magnetostriction, which, for the [111] direction has a saturation value of $\lambda = 5000 \times 10^{-6}$, as large as that of many pure rare

earths at low temperature. This value is also much greater than that of polycrystalline $TbFe_2$ as reported by Clark and Belson[21] (approximately 2000 x 10^{-6}). Since terbium and erbium are expected to contribute to the total magnetostriction with opposite signs, this large value for the ternary crystal is surprising.

These results are quite preliminary, and they have not been fully analyzed. They are presented here as an example of interesting and new results which will probably not be extended or further analyzed because of total lack of funding for this entire line of research.

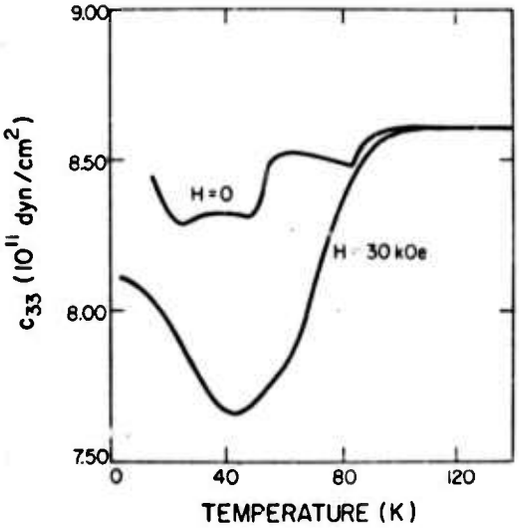

Fig. 33 Temperature dependence of the elastic constant c_{33} of single-crystal erbium in zero applied field and in a 30-kG c-axis field.

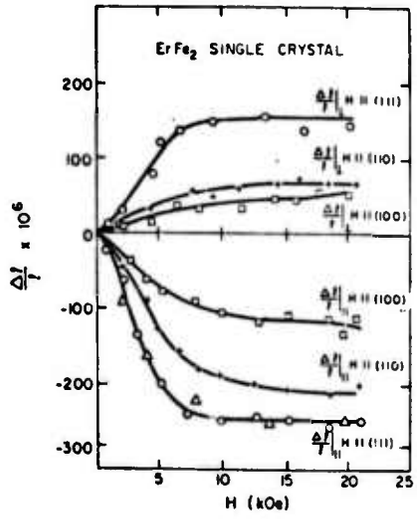

Fig. 34 Magnetostriction of Single-Crystal $ErFe_2$ at room temperature

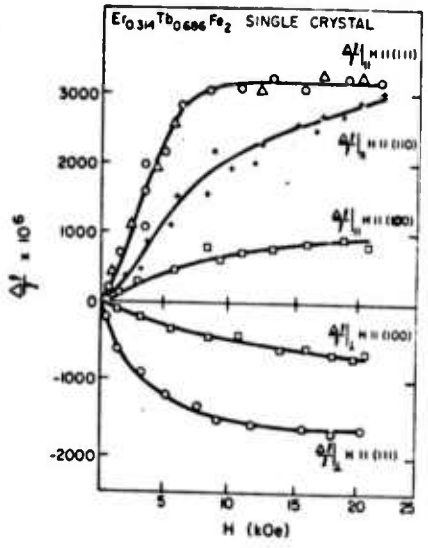

Fig. 35 Magnetostriction of single-crystal $Er_{0.314}Tb_{0.686}Fe_2$ at room temperature.

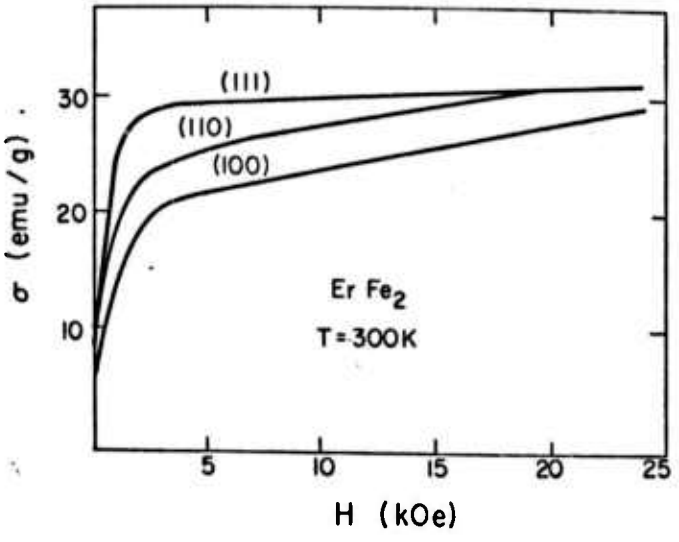

Fig. 36 Magnetization of $ErFe_2$ at room temperature.

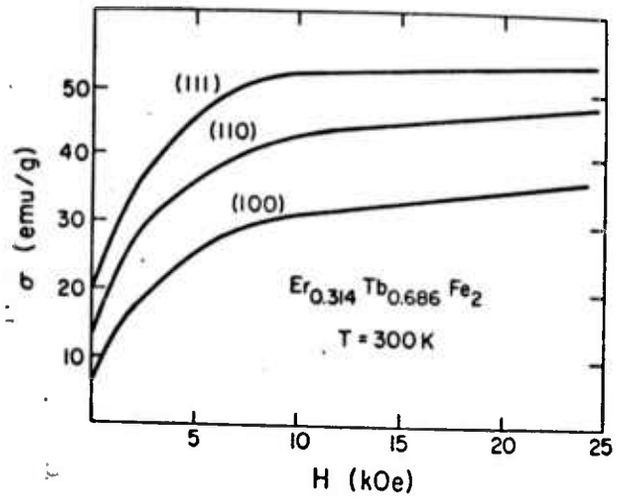

Fig. 37 Room temperature magnetization of $Er_{0.314}Tb_{0.686}Fe_2$.

IV. CONCLUSION

This report has presented a number of aspects of the dynamical magnetoelastic properties of rare-earth materials. It will be noted by the careful reader that in most cases the work is presented in a preliminary or incomplete state. This situation is somewhat unfortunate, but it represents the state of affairs at the time support for this program was terminated. In this program it was necessary to carry out a great amount of preliminary work before results began to come in. During the last year of the project, as can be seen, there were numerous projects in operation, all of which were left with much work remaining to be finished when funds for the support of this work were terminated. It will, of course, be possible to carry on with the analysis of many of these results without financial support, but it will be quite some time before all these results are completely analyzed and a final attempt is made to arrive at a complete and coherent picture of dynamic magnetoelastic interactions in rare-earth materials.

APPENDIX I DEFINITION OF IRREDUCIBLE-TENSOR ANGULAR-MOMENTUM OPERATORS

Since the original introduction by Stevens of the so-called operator equivalents for dealing with problems of crystal fields interacting with magnetic ions in crystal lattices, there have been several conventions for the definition and normalization of these operators, with a certain degree of resulting confusion in the literature. What is proposed here is a simple definition of these operators and a definition which is not only easy to remember but which makes the computation of matrix elements of these operators quite simple. The definitions which follow were inspired by a book of Watanabe[38].

We shall define a set of irreducible-tensor angular-momentum operators of rank ℓ as J_ℓ^m, where m takes on integral values from $-\ell$ to $+\ell$. In order to arrive at a consistent set of operators which can be easily derived at any time, we define the operator J_ℓ^ℓ in the following way:

$$J_\ell^\ell = (-1)^\ell J_+^\ell \quad ; \; J_+ = J_x + iJ_y \tag{AI-1}$$

We then find the remaining operators of this rank by using the basic commutation relations obeyed by any set of irreducible-tensor operators:

$$[\, J_- \, , \, J_\ell^m \,] = \sqrt{\ell(\ell+1) - m(m-1)} \; J_\ell^{(m-1)} \tag{AI-2}$$

With this definition convention, all angular-momentum operators can readily be derived and their matrix elements can easily be evaluated. As an example of the application of the convention, consider:

$$J_1^1 = -J_+ \; ; \; J_1^0 = (2)^{1/2} J_z \; ; \; J_1^{-1} = J_-$$

$$J_2^2 = J_+^2 \; ; \; J_2^1 = -J_+(2J_z + 1) \; ; \; J_2^0 = (2/3)^{1/2}(3J_z^2 - J(J+1))$$

$$J_2^{-2} = J_-^2 \; ; \; J_2^{-1} = J_-(2J_z - 1)$$

The real beauty of this definition becomes apparent when numerical computations must be made, since, if a matrix-oriented computer language such as APL is available, the matrices for all desired irreducible-tensor operators can be obtained with

great ease. The principal advantage in using the definition given here is that it can be remembered easily, and with its use there should never be any uncertainty about the definition or normalization of these operators.

In addition to the basic irreducible tensor operators, which are, of course, given for spherical irreducible representations, it is often necessary to use operators which belong to irreducible representations of lower symmetry. In most cases the following set of Hermitian operators will be useful:

$$J^{+}_{\ell m} = [(-1)^{\ell} J^{m}_{\ell} + J^{-m}_{\ell}]/2 \; ; \; J^{-}_{\ell m} = [(-1)^{\ell} J^{m}_{\ell} - J^{-m}_{\ell}]/2i \; ; \; J_{\ell 0} = J^{0}_{\ell} \; .$$

Examples are:

$$J^{+}_{11} = J_x \; ; \; J^{-}_{11} = J_y \; ; \; J_{10} = J_z \; (2)^{1/2}$$

$$J^{+}_{22} = J^2_x - J^2_y \; ; \; J^{+}_{21} = [J_x J_z + J_z J_x] \; ; \text{ etc.}$$

APPENDIX II IRREDUCIBLE-TENSOR STRAIN COMPONENTS FOR HEXAGONAL SYMMETRY

The simplest choice for the second-rank irreducible-tensor strain components for hexagonal symmetry would appear to be the following:

$$e^{\alpha,0} = e_{xx} + e_{yy} + e_{zz} \; ; \quad e^{\alpha,2} = 3e_{zz} - e^{\alpha,0};$$

$$e^{\gamma}_1 = e_{xx} - e_{yy} \; ; \; e^{\gamma}_2 = e_{xy} + e_{yx} \; ; \; e^{\varepsilon}_1 = e_{xz} + e_{zx} \; ; \; e^{\varepsilon}_2 = e_{yz} + e_{zy}$$

Using other definitions with various multiplicative factors,both rational and irrational, which seem to vary from one author to another, seems to cause confusion and makes it much more difficult to follow through calculations made by different authors. It would appear to be to the advantage of all new workers entering fields where these irreducible-tensor components must be used frequently to standardize the definition, and, in the interests of simplicity, to make such a standard definition as free from confusing factors as possible. Some authors may argus that the multiplicative factors which they happened to use in their definitions of these tensor quantities arise naturally, but there seems to be no evidence to support such a contention.

REFERENCES

1. R. J. Elliott, editor, Magnetic Properties of Rare Earth Metals (Plenum Press, New York 1973).

2. R. S. Tebble and D. J. Craik, Magnetic Materials (Wiley, New York, 1969).

3. E. A. nesbitt and J. H. Wernick, Rare Earth Permanent Magnets, (Academic Press, New York, 1973).

4. P. Chaudhari, J. J. Cuomo, and R. J. Gambino, IBM J. Res. and Dev. 66 (Jan. 1973).

5. A. E. Clark and H. S. Belson, AIP Conf. Proc. 5, 1498 (1972).

6. B. W. Southern and D. A. Goodings, Phys. Rev. B 7, 534 (1973).

7. E. Callen and H. B. Callen, Phys. Rev. 139, A445 (1965).

8. T. J. Moran and B. Luthi, J. Phys. Chem Solids 31, 1735 (1970).

9. B. Luthi, T. J. Moran, and R. J. Pollina, J. PHys. Chem. Solids 31, 1741 (1970).

10. F. Freyne, Phys, Rev. B 5, 1327 (1972).

11.B. W. Southern and DA. A. Goodings, Phys. Rev. B 7, 534 (1973).

12. D. A. Goodings, Proc. IEEE Conf. on Ultrasonics., Nov., 1973, p. 278.

13. T. Nagamiya, in Solid State Physics, ed. by F. Seitz, D. Turnbull, and H. Ehrenreich (Academic Press, New York, 1967) v. 21, p. 319.

14. F. Specht, Phys. Rev. 162, 389 (1967).

15. T. A. Kaplan and D. H. Lyons, Phys. Rev. 129 (2072 (1963).

16. A. R. Mackintosh, in Magnetic Properties of Rare Earth Metals, ed. by R. J. Elliott (Plenum Press, New York, 1972), ch. 5, p. 187.

17. K. W. H. Stevens, Proc. Phys. Soc. 55, 209 (1952).

18. J. J. Rhyne, in Magnetic Properties of Rare Earth Metals, ed. by R. J. Elliott, (Plenum Press, New York, 1972), ch. 4, p. 129.

19. R. L. Melcher, Phys. Rev. Letters 28. 165 (1972).

20. W. F. Brown, Jr., J. Appl. Phys. 36, 994 (1965).

21. A. E. Clark and H. S. Belson, Phys. Rev. B 5, 3642 (1972).

22. S. Legvold, J. Alstad, and J. Rhyne, Phys. Rev. Letters 10, 509 (1963).

23. A. E. Clark, B. F. DeSavage, and R. Bozorth, Phys. Rev. 138, A216 (1965).

24. M. P. Maley, P. L. Donoho, and H. A. Blackstead, J. Appl. Phys. 37, 1006 (1966).

25. P. L. Donoho, L. V. Benningfield, P. K. Wunsch, L. B. McLane, and H. A. Blackstead, AIP Conf. Proc. 10, 769 (1973).

26. K. Salama, F. R. Brotzen, and P. L. Donoho, J. Appl. Phys. 43, 3254 (1972).

27. K. Salama, F. R. Brotzen, and P. L. Doncho, J. Appl. Phys. 44, 180 (1973).

28. W. C. Hubbell, P. L. Donoho, C. L. Melcher, and K. Salama, AIP Conf. Proc. 18, 1263 (1974).

29. M. Long, A. R. Wazzan, and V. R. Stern, Phys. Rev. 178, 775 (1969).

30. M. Rosen and H. Klimker, Phys. Rev. B 1, 3748 (1970).

31. J. W. Cable, E. O. Wollan, W. C. Koehler, and M. K. Wilkinson, Phys. Rev. 140, 1896 (1965).

32. D. E. Hegland, S. Legvold, and F. H. Spedding, Phys. Rev. 131, 158 (1963).

33. A. E. Clark, AIP Conf. Proc. 18, 1015 (1974).

34. A. E. Clark, Naval Ordnance Laboratory, private communication.

35. J. J. Rhyne and S. LEgvold, Phys. Rev. 138, A507 (1965).

36. A. E, Clark and H. S. Belson, AIP Conf. Proc. 10, 749 (1972).

37. J. P. Schroeter, Ph. D. Thesis, Rice University, 1974, unpublished.

38. H. Watanabe, Operator Methods in Ligand-Field Theory (Prentice-Hall, New York, 1966).